Assessing impacts of climate variability and land use/land cover change on the water balance components in the Sahel using Earth observations and hydrological modelling

Bennour, Ali; Jia, Li; Menenti, Massimo; Zheng, Chaolei; Zeng, Yelong; Barnieh, Beatrice Asenso; Jiang, Min

DOI
10.1016/j.ejrh.2023.101370

Publication date
2023

Document Version
Final published version

Published in
Journal of Hydrology: Regional Studies

Journal of Hydrology: Regional Studies 47 (2023) 101370

Contents lists available at ScienceDirect

Journal of Hydrology: Regional Studies

journal homepage: www.elsevier.com/locate/ejrh

Assessing impacts of climate variability and land use/land cover change on the water balance components in the Sahel using Earth observations and hydrological modelling

Ali Bennour[a,b,c], Li Jia[a,*], Massimo Menenti[a,d], Chaolei Zheng[a], Yelong Zeng[a,b], Beatrice Asenso Barnieh[a,e], Min Jiang[a]

[a] State Key Laboratory of Remote Sensing Sciences, Aerospace Information Research Institute, Chinese Academy of Sciences, Beijing 100101, China
[b] University of Chinese Academy of Sciences, Beijing 100045, China
[c] Water Resources Department, Commissariat Regional au Developpement Agricole, Medenine 4100, Tunisia
[d] Faculty of Civil Engineering and Geosciences, Delft University of Technology, Stevinweg 1, 2825 CN Delft, the Netherlands
[e] Earth Observation Research and Innovation Centre (EORIC), University of Energy and Natural Resources, P.O. Box 214, Sunyani, Ghana

A R T I C L E I N F O

Keywords:
African Sahel
SWAT model
Remote sensing
ETMonitor
Soil moisture
LULC change
Climate variability

A B S T R A C T

Study region: Senegal river (SRB), Niger river (NRB), and Lake Chad basins (LCB).
Study focus: We investigated the impacts of land use/land cover change (LULC) and climate variability on the water balance components from 1990 to 2020. We applied the Soil and Water Assessment Tool (SWAT) coupled with remote sensing retrievals of actual evapotranspiration (ETa) and surface soil moisture (SSM). To separate the impacts of the two aforementioned factors, two numerical experiments were designed: (i) climate variability effects by applying frozen LULC while changing the climate; (ii) LULC change impacts by applying frozen climate while changing LULC.
New hydrological insights for the region: Overall, at the basin level, the results indicated that climate variability had the dominant role in increasing groundwater recharge, surface runoff, groundwater return flow and lateral flow in LCB and SRB. These increases triggered the recovery of lake area and higher water table in LCB and increased in SRB streamflow, while water scarcity increased in NRB. In contrast, the separate effect of LULC change, specifically natural vegetation expansion, increased actual ET and decreased the surface runoff, which could be a reason for lake area depletion in LCB and decreasing SRB and NRB streamflow. At the sub-basin level, LULC change, i.e. a gain in cropland and urban areas at the expense of forests in some sub-basins in NRB, led to a local increase in surface runoff. This implies a better redistribution of water in downstream and compensates the deficit in surface runoff caused by natural vegetation expansion in some other catchments. These changes, simultaneously with high intensity and long-duration precipitation, may increase the likelihood of inundation in some small catchments in the Niger river basin. These outcomes give useful hydrological insights into water and land management by emphasizing the crucial role of water recycling.

* Corresponding author.
E-mail address: jiali@aircas.ac.cn (L. Jia).

https://doi.org/10.1016/j.ejrh.2023.101370

Available online 7 April 2023

1. Introduction

Understanding the response of a watershed to climate variability is complex because it is non-linear due to the concurrent response of LULC to the same variability, response modulated by anthropic interventions (Chen et al., 2019; Ewen and Parkin, 1995; Chen and Yu, 2013). The non-linearity is due to the modification of a watershed hydrological properties because of LULC changes. This process is particularly relevant and complex under arid and semi-arid conditions such as in the Sahel, where changes in water availability lead to large and rapid changes in LULC, through the natural response of ecosystems to water and to the efforts of local communities to take advantage of water resources to improve land productivity for better food security. A holistic comprehension of land surface dynamics, its complexity, and the interaction between its different parts are crucial to investigating the water balance components (WBCs) (Feyen and Vázquez, 2011). The effects of LULC change and climate variability on hydrological response could be different across regions (Chu et al., 2010). Therefore, quantifying the impacts of LULC change and climate variability on the water balance of a river basin and its spatial pattern is essential for understanding catchment hydrology (Yin et al., 2017). Moreover, a better understanding of the separate impacts of LULC and climate variability on water balance components is needed to develop effective land management policies towards sustainable water security. The United Nations articulated the Sustainable Development Goals (SDGs) to identify shared priorities towards a better future for all (Scott and Rajabifard, 2017; Vinuesa et al., 2020). Specifically, SDG 6 addresses water security through a detailed hierarchy of Tasks and Targets which may be better achieved by combining land and water management.

These general concepts are even more relevant in Africa, where climate variability is a fundamental challenge, especially in the Sahel region which is considered one of the most vulnerable zones in the world. The Sahel is characterized by a variation in climate from arid in the North to humid in the South (Trémolières, 2010) including hyper-arid, arid, semi-arid, and dry sub-humid zones. Moreover, Niger river, Lake Chad and Senegal river are large basins/lake in the Sahel which provide water resources for livelihood and shared by several countries. This led to establish multiple organizations and communities to manage water resources (Trémolières, 2010), which further enhances the relevance of these basins for a study of the response to climate variability and LULC changes. The three basins are characterized by a large N–S gradient in annual precipitation, approximately ranging from 100 mm a^{-1} in the northern upper reaches to 1500 mm a^{-1} in the southern lower reaches.

The three aforementioned basins in the Sahel experienced an important variability in precipitation since the 1970 s drought. In the western part of the Sahel region, the Senegal basin showed an increase in mean annual rainfall. Bodian et al. (2020) stated that the average annual precipitation between 1940 and 2013 was about 500 mm, while Karambiri et al. (2011) reported that the mean annual precipitation in 1990 was about 550 mm. This increase in precipitation was confirmed by other studies (Anyamba and Tucker, 2005; Olsson et al., 2005). The Niger river experienced a variability in rainfall, especially after the 1970 s drought. For instance, Descroix et al. (2012) stated that the mean rainfall from 1905 to 2003 ranged between 300 mm and 570 mm. while Sighomnou et al. (2013) reported that the mean rainfall during 1950–2013 was about 551 mm, and many other studies reported a decrease in precipitation during recent years in the Niger basin (Hulme, 2001; Okpara et al., 2013). On the other hand, the Lake Chad basin experienced an increase in precipitation as reported by Nkiaka et al. (2017) and Okonkwo et al. (2014). The mean annual rainfall in Lake Chad basin between 1951 and 2013 was about 465 mm (Mahmood and Jia, 2019). Thus, climate variability in the three watersheds was characterized by a different rainfall trend from West to East. This variability in precipitation may have different impacts on hydrological responses in the three basins. Likewise, LULC was rather different, with cropland covering about 30% of the Niger basin, while being less than 10% in the Senegal basin. Additionally, natural vegetation was more expanded in Senegal river and Chad Lake basins covering 80% while only 50% in the Niger river basin. Some noticeable LULC transitions were detected by other studies in Senegal basin, for instance the gain of urban area and the cropland loss (Barnieh et al., 2020; Nwilo et al., 2020). Contrariwise, an increase in cropland was stated in Niger basin (Barnieh et al., 2020; Nwilo et al., 2020). On the other hand, the Lake Chad basin experienced water bodies loss and crop land increase at the expense of wetland (Barnieh et al., 2020). Accordingly, we choose these three basins for detailed case-studies.

Several studies paid attention to investigating the effects of LULC change and climate variability on hydrological response in the Sahel region. For instance, Albergel (1987) investigated the impact of the 1970 s drought on surface runoff in two small catchments in the Sahel (22 and 54 Km^2). His study reported that the surface runoff increased, despite the precipitation decrease. He attributed this increase to soil degradation caused by agriculture expansion. This hypothesis was also reported by other studies (Mahe and Olivry, 1999). Mahe (2006) studied the hydrological response to LULC changes in several small catchments in the Sahel. They reported that the expansion of cultivated area after deforestation since the 1970 s led to a decline in soil infiltration capacity and an increase in surface runoff. Leduc et al. (2001) and Leblanc et al. (2008) have investigated the impacts of natural vegetation clearing on surface runoff and groundwater recharge in different small catchments in the Sahel. They reported that the natural vegetation clearing led to an increase in surface runoff, with the being accumulated in ponds where it infiltrated to the aquifer. Mahe et al. (2011) have investigated the hydrological response to climate and LULC change in different sub-basins in the Niger River basin during and after the 1970 s drought. They stated that an increase in surface runoff has occurred despite the deficit in rainfall, and they attributed this increase to deforestation. This increase in surface runoff due to deforestation, vegetation clearing and cultivated area expansion despite rainfall deficit was later defined as the first Sahelian Hydrological paradox (Descroix et al., 2013). More recently, rainfall and vegetation recovery was reported in several studies (Ali and Lebel, 2009; Anyamba and Tucker, 2005; Brandt et al., 2017; Descroix et al., 2015; Fensholt and Rasmussen, 2011; Jiang et al., 2022). After the precipitation recovery and the re-greening of the Sahel region, many studies have been done to investigate the impacts of both LULC change and climate variability on hydrological response. Mahe et al. (2003) investigated the evolution of surface runoff in several small catchments of right bank tributaries of the middle Niger river and found that the surface runoff did not decrease despite the deficit in rainfall and they attributed this increase to cropland expansion. Amogu et al. (2015) studied the impacts of cropped area on surface runoff in two small Sahelian catchments in the Niger river basin.

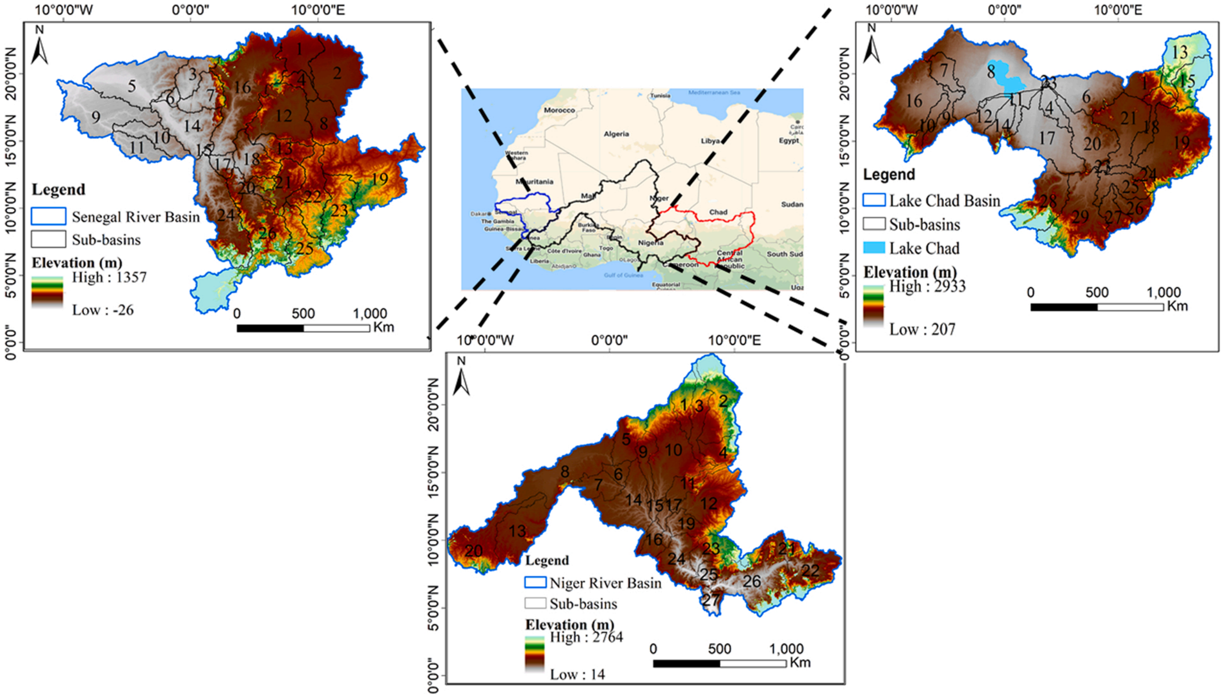

Fig. 1. Location map of the three basins in the Sahel region, i.e., Senegal River, Niger River and Lake Chad basins.

They found that the cropland changed soil characteristics, which led to an increase in surface runoff. In Gourma in Mali, Dardel et al. (2014) have investigated the impact of vegetation recovery and climate variability on surface runoff from 1980 to 2012. They have used remote sensing data and ground observations. Furthermore, Nka et al. (2015) have used hydrological ground observations to investigate the relationship between the increase in floods occurrence and climate variability in 11 small catchments (area ranging between 1750 and 12,200 km^2) in the Sahel. They found that the increase in the occurrence of floods in these 11 catchment was due to climate variability, while no impact of LULC change was detected. Other studies have investigated the relationship between climate and LULC changes and hydrological response in the Sahel (Descroix et al., 2012; Descroix et al., 2009) and they attributed the increase in surface runoff to LULC change particularly crop land expansion. While some other studies reported that it is difficult to determine whether the increase in surface runoff was due to LULC change or climate variability, but it is a result of combined factors (Mahé and Paturel, 2009). The increase in runoff, which has been occurring after vegetation recovery, has recently been defined as the second "Sahelian paradox" (Dardel et al., 2014). Almost of all previous studies have investigated the impacts of LULC change and climate variability on water balance in the entire region or in a huge area using statistical techniques based on a combination of remote sensing data (NDVI) and ground observations data (precipitation and surface runoff). These two types of data do provide the information necessary to separate the impacts of the two studied factors. Some other studies have applied hydrological models to separate the contribution of the two factors in changing hydrological response but in small catchments (<1000 km^2). Furthermore, most of the studies focused on surface runoff and streamflow, while other water balance components are important but not well studied such as groundwater recharge and groundwater return flow. Moreover, water recycling as a consequence of LULC change was not evaluated. Most studies compared the drought period (1970 s and 1980 s) with the years past the drought till 2010. A study at basin level and sub-basin level, after the last recovery of vegetation and rainfall, has not been done yet. Furthermore, it is quite important to quantify the separate contributions of LULC change and climate variability in changing the water balance components.

Based on the literature, the Sahel region is experiencing a rainfall recovery accompanied by re-greening due to the expansion of cropland and natural vegetation, which increased water consumption. These changes in LULC present a huge environmental challenge for Sahelian water resources. So LULC change combined with climate variability raised serious threats for the hydrological response of this region, which must be studied.

Thus, the objectives of this study are 1) to evaluate the separate impacts of climate variability and LULC on water balance components using a physically-based hydrological model; 2) to estimate the responses of different water balance components to climate variability and LULC changes at basin and sub-basin scale; and 3) to compare the relative contributions of these different factors and identify which one has the dominant impacts. All abbreviations used in this study are defined in Table A1.

The novelty of this study is to separate and assess the impacts of LULC changes and climate variability on the water balance of large catchments, particularly the quantification of groundwater recharge, water recycling, and the validity of the first and second hydrological paradox, specifically in the NRB. Further, we analyzed in-depth the impacts of LULC change and climate variability on the water balance of sub-catchments to identify the impacts of specific LULC changes, e.g., cropped area in NRB on the water balance during post-drought (1990–2000), near post-drought (2001–2010) and far post-drought (2010–2020). Besides, verifying the two aforementioned paradoxical behaviors was done at the sub-basin level.

2. Study area and data

2.1. Study area: African Sahel

The Sahel is characterized by four climatic zones: hyper-arid, arid, semi-arid, and dry sub-humid. Several large hydrological basins are located in the Sahel, e.g., Lake Chad, Senegal and Niger river basins. This transition area attracted scientific attention due to the noticeable changes in climate and LULC during the last decades and their complex relationship with the hydrological response and water resources. The first and second hydrological paradoxes were suggested in the Sahel (Casenave and Valentin, 1992; Descroix et al., 2018). The Lake Chad basin, which was the largest endorheic basin in the world, experienced dramatic changes in terms of water area. The Lake changed from large (24,000 km^2) to normal or intermediate (18,000 km^2) and finally to a small lake fragmented into different separated water bodies as a permanent open water pool (1700 km^2) and permanent or seasonal marshes (from 2000 to 14, 000 km^2) (Lemoalle et al., 2012). The largest basin in terms of catchment area in the Sahel and the third longest river in Africa is the Niger, which is characterized by the Niger River Inland Delta and Lakes District (Andersen et al., 2012). The latter is a huge wetland in the basin, and its tributaries along the Middle Niger Left-Bank are sensitive to climate variability and LULC changes (Andersen et al., 2012; Descroix et al., 2009; Rameshwaran et al., 2021). The Senegal River basin experienced noticeable variations in hydrological responses due to intensive changes in LULC as well as climate variability, specifically the precipitation (Faty et al., 2019; Oyebande and Odunuga, 2010). These three huge basins represent an important topic of studies addressing LULC changes, climate variability, and hydrological responses.

2.1.1. Basin level

2.1.1.1. Senegal River Basin (SRB). The Senegal River basin (SRB) (Fig. 1) is located in the western part of the Sahel region, with a total drainage area of approximately 375,000 Km^2 and a length of 1800 km. The region is inhabited by 3.5 million people. The basin is shared by four countries, Senegal, Guinea, Mali, and Mauritania. The rainfall in SRB varies from less than 200 mm to the North to about 2000 mm in the South, and it is characterized by a rainy season from July to October. The SRB experienced a severe drought for about 30 years since 1970. Almost all previous studies in the Senegal basin focused on the variation of streamflow and surface runoff and led to conclude that rainfall is the main driver of surface runoff and streamflow variation. On the other hand, the quantification of groundwater recharge, as well as surface runoff, lateral flow and groundwater return flow and their contribution to water recycling within the watershed, were less studied. Further, the role of LULC changes and the effects on water balance components has not been deeply investigated.

Senegal river basin experienced a conversion of crop land to other vegetation (natural vegetation) from 1975 to 2013 (Barnieh et al., 2020), who also reported a gain in urban area. Likewise, the transition from cropland to other vegetation was also detected in the Senegal basin (Barnieh et al., 2020). Additionally, water bodies' loss was balanced by gains in other vegetation and wetland. Moreover, an increase in urban area, cropland and grassland between 2009 and 2018 was detected (Faye and Du, 2021). Vittek et al. (2014) have reported that from 1975 to 1990, other vegetation increased at the expanse of tree cover, most probably due to agricultural expansion.

2.1.1.2. Niger River Basin (NRB). The Niger River (Fig. 1) has a catchment area of 2.1 $\times$ 10^6 km^2 and a length of 4200 km. This region is inhabited by more than 100 million people and spans nine countries. The rainfall in NRB varies from less than 200 mm in the North to about 2000 mm in the South, and it is characterized by a rainy season from July to October. A severe and extended drought has occurred in the watershed since 1970. Almost all previous studies in the Niger basin focused on the variation of streamflow and surface runoff. They reported that during the aforementioned drought, a first hydrological paradox was suggested in this basin, i.e., the increase in surface runoff despite the decrease in rainfall (Descroix et al., 2013). Furthermore, other studies reported that in the post-drought period, characterized by precipitation and vegetation recovery, a second hydrological paradox appeared: despite the increase in vegetation cover, the surface runoff did not show any change. The impacts of the vegetation and precipitation recovery were insufficiently investigated, especially separating the impacts of these two factors. On the other hand, the hydrological responses to changes in LULC and climate variability, particularly the validity of the hydrological paradoxes at the basin and sub-basin level has not been thoroughly evaluated. It can be considered a gap in hydrological knowledge in this important basin.

The Niger basin experienced an increase in agricultural crops at the expense of other vegetation and forest as reported by (Barnieh et al., 2020). Vittek et al. (2014) have reported that from 1975 to 1990, other vegetation increased at the expense of tree cover, most probably due to agricultural expansion. Also, Obahoundje and Diedhiou (2022) and Descroix et al. (2013) sta documented an expansion of agriculture in the Niger basin and the loss of water bodies to cropland in the Niger delta.

2.1.1.3. Lake Chad Basin (LCB). The Lake Chad basin (LCB) is the largest endorheic lake basin in the world, and it is located in the center of the African Sahel between 5.19° and 25.29°N latitude and 6.85–24.45°E longitude with an area of 2.5 $\times$ 10^6 km^2. The region is inhabited by 17.4 million people. According to (Delclaux et al., 2008), the northern part of the basin is located in the Sahara, and it does not generate runoff, so in this study, we consider only the southern part (Fig. 1). The southern part of LCB is covering an area of 1 10^6 km^2. (Fig. 1) and is shared by ten countries. The open water area has experienced dramatic changes due to the severe drought since 1970 from large (24,000 km^2) to normal or intermediate (18,000 km^2) and finally to a small lake fragmented into different separated

Table 1
Description of forcing data used in the SWAT model and earth observation data used for model calibration and validation in this study.

Variables	Temporal coverage	Spatial Resolution	Products Source/reference
DEM	-	30 m	Shuttle Radar Topography Mission (SRTM) 30 m Digital Elevation Data (www.earthexplorer.usgs.gov)
Soil	-	1 km	Digital Soil Map of the World (DSMW) version 3.6: Land and Water Development Division, FAO, Rome
LULC	1990–2010 and 2020	30 m	LULC product access: https://doi.org/10.11888/Terre.tpdc.272021, (Yu, 2022)
Precipitation	1981–2021	5 km	Climate Hazards Group Infrared Precipitation with Station data (CHIRPS): https://data.chc.ucsb.edu/products/CHIRPS-2.0/global_daily/tifs/p05/
Min/Max Temperature Wind speed Relative humidity Solar radiation	1950–2021	31 km	the European Centre for Medium-Range Weather Forecasts (ECMWF ERA5) reanalysis (Hersbach et al., 2020)
Actual evapotranspiration	2001–2020	1 km	ETMonitor ET Product, access: https://doi.org/10.11888/RemoteSen.tpdc.272831, https://doi.org//10.12237/casearth.6253cddc819aec49731a4bc2, (Zheng et al., 2022)
Soil moisture	2002–present	36 km	NN Soil Moisture Product, access: https://doi.org/10.11888/Terre.tpdc.271954, (Yao et al., 2021)

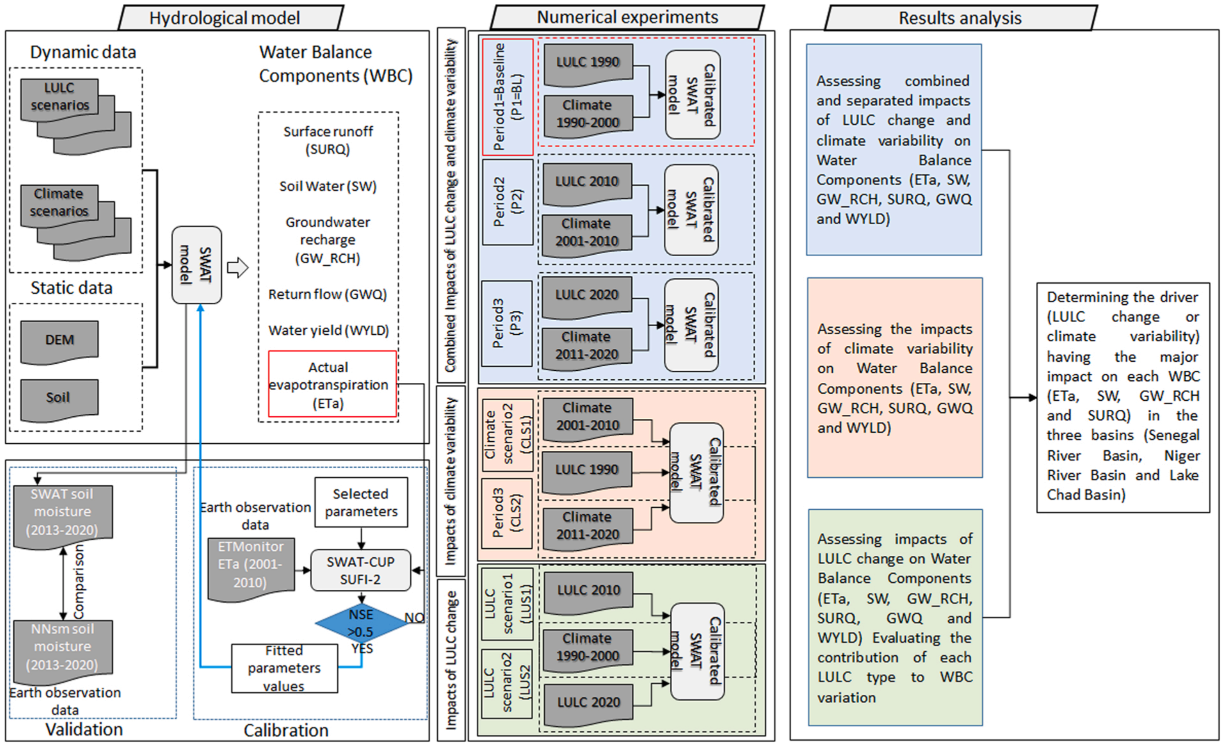

Fig. 2. Study workflow: 1) Hydrological modeling including Calibration/Validation of SWAT model; 2) Numerical Experiments including assessment of the combined impact of LULC and climate change, the impact only by climate change and the impact only by LULC change on each of the simulates water balance components; 3) Results Analysis.

water bodies as a permanent open water pool (1700 km^2) and permanent or seasonal marshes (from 2000 to 14,000 km^2) (Lemoalle et al., 2012). The rainfall in the LCB varies from less than 100 mm in the North to about 1000 mm in the South, and it is characterized by a rainy season from July to September. Almost all previous studies in the Lake Chad basin focused on investigating the variation of surface runoff during the drought and post-drought periods, evaluating at the same time the impacts of LULC changes and climate variability mainly on surface runoff (Mahmood and Jia, 2019; Zhu et al., 2019). Furthermore, some studies have assessed the impacts of climate change on the lake water balance and reported that groundwater is the main contributor to lake seepage (Pham-Duc et al., 2020). The groundwater recharge and its role in the lake water balance were insufficiently taken into account and water recycling within the LCB, particularly as a consequence of LULC changes, was not studied.

The major LULC changes in LCB from 1975 to 2013 stated by (Barnieh et al., 2020) were the transition of water bodies and wetland around the Lake to cropland, the loss of water bodies to other vegetation and an increase in urban area at the expense of other vegetation. In 1975–1990, other vegetation increased at the expense of tree cover, most probably due to agricultural expansion (Vittek et al., 2014). An increase in cropland at the expense of other vegetation was reported by Nwilo et al. (2020).

2.1.2. Sub-basin selection

To illustrate the impact of LULC changes in the Sahel, we have selected several sub-basins as hotspots in terms of LULC transitions. At the basin level, the major transition in the three watersheds was from bare land and forest to natural vegetation (grass and shrub lands). At the sub-basin level, and based on the (LULC) transition matrix in each sub-basin, we have considered only one example of each unique transition from one LULC class to another, i.e. if we have 10 sub-basins characterized by a transition from bare land to grassland, we choose one example of these 10 etc. Accordingly, the selected sub-basins were:

- From forest to cropland in sub-basin 24 in Niger River Basin (NRB_sub24);
- From forest to urban and grassland in sub-basin 23 in Niger River Basin (NRB_sub23);
- From bare land to grassland in sub-basin 4 in Senegal River Basin (SRB_sub 4);
- From grassland and cropland to water in sub-basin 8 in Lake Chad Basin (LCB_sub8);
- From forest and grassland to shrub land, cropland, and urban in sub-basin 29 in Lake Chad Basin (LCB_sub29).

2.2. Data

This study used several datasets to drive the SWAT model, listed in Table 1. Brief description of these data is given below, readers may refer to the relevant references for more details. This study covers the period of 1990–2020.

The precipitation data were from the Climate Hazards Group Infrared Precipitation with Station (CHIRPS). The data was used at daily time steps from 1988 to 2020. Atmospheric data, including daily minimum and maximum temperature, relative humidity, wind speed, and solar radiation data were extracted from the fifth-generation European Centre for Medium-Range Weather Forecasts reanalysis data set (ECMWF ERA5) (Hersbach et al., 2020). This data were used at the daily time step. The land use and land cover (LULC) dataset used in this study were produced by the Tsinghua University based on Landsat data at a spatial resolution of 30 m (Feng, 2018; Xu, 2018; Zhao, 2021), and available for 1990, 1995, 2000, 2005, 2010, 2015, and 2020. We have used only three years: 1990, 2010, and 2020 to quantify the impacts of LULC changes on water balance. The soil data set was obtained from the Digital Soil Map of the World (DSMW) version 3.6 produced by the Food and Agriculture Organization (FAO) at a 1 km resolution. The physical properties were extracted for each soil texture class from the SWAT database Map Window (MW) interface (http://swat.tamu.edu/-software/mwswat/). The data set on soil properties is compiled from FAO world soil data. The Digital elevation model (DEM) of LCB was clipped out of the Shuttle Radar Topography Mission (SRTM) 30 m resolution Digital Elevation Data (www.earthexplorer.usgs.gov).

Following our previous study (Bennour et al., 2022), the ETMonitor global ET product (Hu and Jia, 2015; Zheng et al., 2022; Jia et al., 2018) was used to calibrate the SWAT model.

The validation of SWAT mode simulations was done using remote sensing retrievals of soil moisture generated by Yao et al. (2021) applying a neural network algorithm (NNsm). The NNsm dataset was downloaded from: http://data.tpdc.ac.cn/en/data/c26201fc-526c-465d-bae7–5f02fa49d738/.

Due to the different ways of calculating soil moisture, i.e., SWAT, which simulates surface soil moisture based on an empirical equation and different remote sensing algorithms such as random forest to generate surface soil moisture, a systematic bias correction was applied using the mean–standard deviation (μ − σ) matching (linear regression) technique (Draper et al., 2009; Lopez et al., 2017; Rajib et al., 2016). The correction was done based on the following equation:

$$\theta'_{SWAT} = [(\theta_{SWAT} - M_{SWAT}) * (\sigma_{RS}/\sigma_{SWAT})] + M_{RS} \quad (1)$$

where θ'_{SWAT} and θ_{SWAT} are corrected and original soil moisture, respectively; $M_{RS,}$ and M_{SWAT} are the mean of soil moisture from remote sensing and SWAT; σ_{SWAT} and σ_{RS} are the standard deviation of SWAT and remote sensing soil moisture, respectively.

3. Methodology

Generally, the approach used in this study (Fig. 2) is based on designing and carrying out simulation experiments to assess the individual and combined impacts of LULC change and climate variability on different water balance components of the three basins described in Section 2 for the period of 1990–2020. The hydrological model SWAT was applied to estimate water balance components (WBCs) for the designed experimental scenarios: changing LULC alone, changing climate condition alone, and the combined changes of these two factors. The results of the numerical simulations were analyzed to identify the dominant drivers of the changes in water balance components in the study area.

In this work, the study period was split into three periods, i.e., the post-drought period (1990–2000), the near post-drought (2001–2010) and the far post-drought period (2010–2020), based on precipitation evolution in the three watersheds. The hydrological responses to LULC changes and climate variability were assessed during the near post-drought (2001–2010). In this period, the rainfall decreased in both Niger river and Lake Chad basins, while it increased in the Senegal river basin compared to the post-drought period (1990–2000). During the far post-drought period (2010–2020), rainfall increased in both Lake Chad and Senegal river basins, while it decreased steadily in the Niger river basin, compared with the post-drought period (Fig. A1). These different rainfall trends might have had different impacts on the water balance of basins and sub-basins.

Before carrying out the numerical simulation experiments, the SWAT model was calibrated using actual evapotranspiration (ET) data derived from remote sensing product based on ETMonitor model (Bennour et al., 2022). For validation, the soil moisture simulated by the calibrated SWAT model was evaluated by comparing with the remote sensing product of surface soil moisture (Fig. 2).

The following sections describe the different steps of the approach.

3.1. SWAT model description

3.1.1. SWAT model set-up

The hydrological model SWAT used in this study is an open-source and semi-distributed model (Arnold et al., 1998). The model is forced by data on meteorology, topography, soil properties and LULC, and runs on a daily time step to simulate the water balance components in a watershed. In this study, the ArcSWAT2012 version (Winchell et al., 2013) was set up in the Lake Chad basin, Niger and Senegal river basins based on a 30 m resolution Digital Elevation Model (DEM). Then, these three watersheds were disaggregated into sub-basins, which were further divided into Hydrological Response Units (HRU-s) which are the smallest units in the watershed and that are comprised of unique LULC, soil and slope combinations (Neitsch et al., 2011). The SWAT model is not a fully distributed model, and the disaggregation of the domain into sub-basins and HRU-s is required to preserve the natural flow paths, boundaries, and channels required for routing water, sediments, and pollutants. The disaggregation is done by applying a watershed discretization technique based on topographic features (Neitsch et al., 2011). The number of sub-basins is determined by the size of the watershed and the spatial resolution of the digital elevation model used for this purpose (Neitsch et al., 2011). In this paper, the watersheds were

Table 2
The 16 parameters applied in the calibration with estimated range and fitted values in this study.

Parameters	Description	Ranges		Fitted values		
		min	max	SRB	NRB	LCB
r_CN2	SCS runoff curve number f	-0.5	0.85	0.13	0.09	0.10
v_ESCO	Soil evaporation compensation factor	0.25	0.95	0.57	0.42	0.36
r_SOL_AWC	Available water capacity of the soil layer	-0.25	0.95	-0.14	0.59	0.45
r_SOL_Z	Depth from soil surface to bottom of layer	0	0.2	0.30	0.37	0.30
r_SOL_K	Saturated hydraulic conductivity	-0.4	0.95	0.40	0.81	0.90
r_SOL_BD	Moist bulk density	-0.4	0.95	0.15	0.19	0.17
v_FFCB	Initial soil water storage expressed as a fraction of field capacity water content	0	1	0.54	0.05	0.54
v_EPCO	Plant uptake compensation factor	0	1	0.65	0.19	0.10
v_FLOWFR	Fraction of available flow	0	1	0.50	0.79	0.86
r_SOL_ZMX	Maximum rooting depth of soil profile	0.2	0.8	0.43	0.75	0.35
v_GSI	Max stomatal conductance	0	5	0.89	1.04	3.05
v_GW_DELAY	Groundwater delay (days)	0	500	47.80	417.47	175.67
v_TDRAIN	Time to drain soil to field capacity	0	72	70.71	35.85	55.01
v_SLSOIL	Slope length for lateral subsurface flow	0	150	3.56	22.81	60.29
v_SURLAG	Surface runoff lag time	0.05	24	8.82	19.73	6.82
v_BLAI	Max leaf area index	0.5	10	3.26	4.98	4.93

Table 3
Metrics were applied to evaluate the calibration and validation.

Performance metrics	Equations	Descriptions
Coefficient of determination	$R^2 = \frac{[\sum_i (ET_{Rs,i} - \overline{ET_{Rs}})(ET_{s,i} - \overline{ET_s})]^2}{\sum_i (ET_{s,i} - \overline{ET_s})^2 \sum_i (ET_{Rs,i} - \overline{ET_{Rs}})^2}$	Where: ET_{Rs} represents satellite-based ETa values; ET_s represents SWAT simulates ET values; $\overline{ET_{Rs}}$ represents mean satellite-based ET values; $\overline{ET_s}$ represents mean simulated ET values. r is the Pearson product correlation coefficient between satellite-based ET and the simulated ET;
Nash-Sutcliffe Efficiency	$NSE = 1 - \frac{\sum_i (ET_{Rs} - ET_s)_i^2}{\sum_i (ET_{s,i} - \overline{ET_s})^2}$	α is the standard deviation of the simulated ET over the standard deviation of the satellite-based ET, β is the ratio of the mean simulated ET to the satellite-based ET.
Kling-Gupta Efficiency	$KGE = 1 - \sqrt{(r-1)^2(\alpha-1)^2(\beta-1)^2}$	
Percent Bias	$PBIAS = \frac{\sum_{i=1}^{n}(ET_{Rs} - ET_s)i}{\sum_{i=1}^{n}(ET_{Rs})}$	

delineated and divided into 29, 27, and 26 sub-basins for Lake Chad basin, Niger and Senegal river basins, respectively.

The catchment water balance calculation in the SWAT model is based on the principle of mass conservation:

$$SW_t = SW_0 + \sum_{i=1}^{N}(PRECIP_i - SURQ_i - ET_{ai} - GWRCH_i - GWQ_i) \tag{2}$$

where t is the ending day of numerical simulation, N is the duration of the numerical experiment (i.e. total days of simulation), the subscript i is the day number (i = 1,2,3, …, N), SW_t is the final soil water content for the entire soil profile (mm) of the whole simulation period, SW_0 is the initial soil water content (mm), $PRECIP$ is the precipitation (mm), $SURQ$ is the surface runoff (mm), $ET_{a,i}$ is the actual evapotranspiration (mm), $GWRCH$ is the groundwater recharge (water entering the vadose zone from the soil profile) (mm) and GWQ is the groundwater return flow (mm). The simulation was done at daily step, all variables in Eq. (2) are daily values.

3.1.2. An indicator of water recycling: the ratio of water outflow to water inflow

It is interesting to introduce anthropic water diversions for different uses and inter-basin water transfer, which would modify the natural response of the basins. However, due to lack of information of where such interventions were applied, it is impossible to introduce precisely such anthropic interventions on water flows. The SWAT computes the contributions of each sub-basin to streamflow, i.e. WYLD = SURQ+LATQ+GWQ, then provides options to describe the use of streamflow in the river channels (i.e. diversions for irrigation or other uses) and allows inter-sub-basin water transfers (Neitsch et al., 2011). We proposed to use the ratio of WYLD/PREC as an indicator for potential water recycling, i.e. the ratio of out/in-recycling (R_{oiR}), calculated as:

$$R_{oiR} = WYLD/PREC \tag{3}$$

where R_{oiR} is the ratio of out/in recycling, $PREC$ is the sum of precipitation over all sub-basins (km^3), $WYLD$ (km^3) is the net amount of water that leaves the sub-basin and contributes to streamflow in the reach and calculated as:

$$WYLD = SURQ + LATQ + GWQ - Q\_TLOSS \quad (4)$$

where $LATQ$ (km^3) is the lateral flow contribution to streamflow; and Q_TLOSS (km^3) is the transmission loss.

3.1.3. SWAT model calibration and validation

As in-situ data were not available from the three basins, the SWAT model calibration was conducted using actual evapotranspiration data derived from remote sensing observations following the calibration approach in our earlier work (Bennour et al., 2022), instead of using run-off data as usually done. Specifically, the SWAT model was calibrated based on ETMonitor actual ET (Zheng et al., 2022) for 2001 − 2010 at a monthly time step using SWAT-CUP (Abbaspour, 2015). Table 2 gave the results of the calibrated parameters, the details about the parameter selection and calibration procedure can be found in Bennour et al. (2022).

The validation was done by comparing the simulated soil moisture by the calibrated SWAT model with surface soil moisture derived from satellite remote sensing observations developed by Yao et al. (2021) (called Neural Network soil moisture product (NNSM), see Table 1) from 2013 to 2020 at a monthly time step.

Model calibration and validation were evaluated by applying well documented metrics, i.e., coefficient of determination (R^2), Nash-Sutcliffe Efficiency (NSE), Kling-Gupta Efficiency (KGE), and Percent Bias (PBIAS), according to Moriasi et al. (2007, 2015). All performance metrics used in this study are described in Table 3.

3.2. Design of numerical simulations for assessing impacts of LULC changes and climate variability on water balance components

3.2.1. Design of numerical simulations

To investigate the dominant drivers influencing the water balance components in the three basins of the Sahel, we proposed an approach by carrying out the numerical simulations (experiments) based on scenarios that 1) the combined changes of these two factors, 2) changing climate condition alone, 3) changing LULC alone. Considering that the LULC data are available in 1990–2020, the study period (1990–2020) was split into three sub-periods: period 1 (P1) was in 1990–2000, also taken as the baseline (BL) period, i.e. P1 = BL; period 2 (P2) was in 2001–2010; and period 3 (P3) was in 2011–2020. Forced by the daily meteorological (and precipitation) data and the corresponding LULC data, the calibrated SWAT model was run at a daily step in 1990–2020. The years of 1988 and 1989 were used as a spin-up period. The daily outputs of the simulated water balance components, i.e., surface runoff (SURQ), actual evapotranspiration (ETa), soil water (SW), groundwater recharge (GW_RCH), groundwater return flow (GWQ) and water yield (WYLD), were then integrated to obtain the annual total values for each year which was further averaged over each period to get the 10-year mean of the water balance components of the corresponding period. Spatially, the SWAT model was run in each HRU, then aggregated to obtain values of water balance components at the sub-basin scale and finally the values at basin scale.

Scenarios experiments were designed to identify the impact roles of LULC changes and climate variability, these experiments were carried out by taking corresponding conditions of LULC and climate and described below:

(1) The combined impacts by LULC change and climate variability on WBCs

Numerical simulation was conducted by running the calibrated SWAT model forced by the daily meteorological (and precipitation) data from EAR5 (and CHIRPS) between 1990 and 2020, and the LULC data of 1990, 2010 and 2020 were used to embody the LULC conditions for each one of the three periods (P1: 1990–2000; P2: 2001–2010; P3: 2011–2020). The simulated results of the mean values of annual water balance components in the baseline period (P1 = BL: 1990–2000) were taken as the reference (referred to as baseline values), the mean values of annual water balance components in the other two periods (P2: 2001–2010; P3: 2011–2020) were compared with the baseline values following the equation below:

$$\Delta WBC_{Pi} = WBC_{Pi} - WBC_{BL} \quad (5)$$

where ΔWBC_{Pi} is the change in a water balance component between the corresponding period (Pi = P2 or P3) and the baseline period (P1), WBC_{Pi} is the value of the water balance component in the corresponding period, WBC_{BL} is the value of the water balance component in the baseline period. This experiment (Eq. (5)) gave the results of the combined impact of the actual conditions of LULC changes and climate variability in the two periods of 2001–2010 and 2011–2020, because the impacts were not distinguished.

(2) Impacts of climate variability on WBCs

To evaluate the impacts of the climate variability alone on the WBC, we assumed no change in LULC condition for the entire period in 1990–2020 (frozen as the condition in 1990). The SWAT model was run by taking LULC in 1990 and actual daily meteorological (and precipitation) data in 1990–2020. We divided the period of 2001–2020 into two climate scenarios: 2001–2010 as climate scenario 1 (CLS1), 2011–2020 as climate scenario 1 (CLS2). The impact of climate variability on a WBC in each climate scenario period was calculated as:

$$\Delta \mathrm{WBC}_{CLi} = WBC_{CLSi} - WBC_{BL} \quad (6)$$

where $\Delta \mathrm{WBC}_{CLi}$ is the change in a water balance component between the corresponding period (CLS1 or CLS2) and the baseline period, WBC_{CLSi} is the value of the water balance component for either CLS1 or CLS2, WBC_{BL} is the value of a water balance component in the baseline period. This experiment (Eq. (6)) gave the results of impact by climate variability only during the two periods of 2001–2010 and 2011–2020.

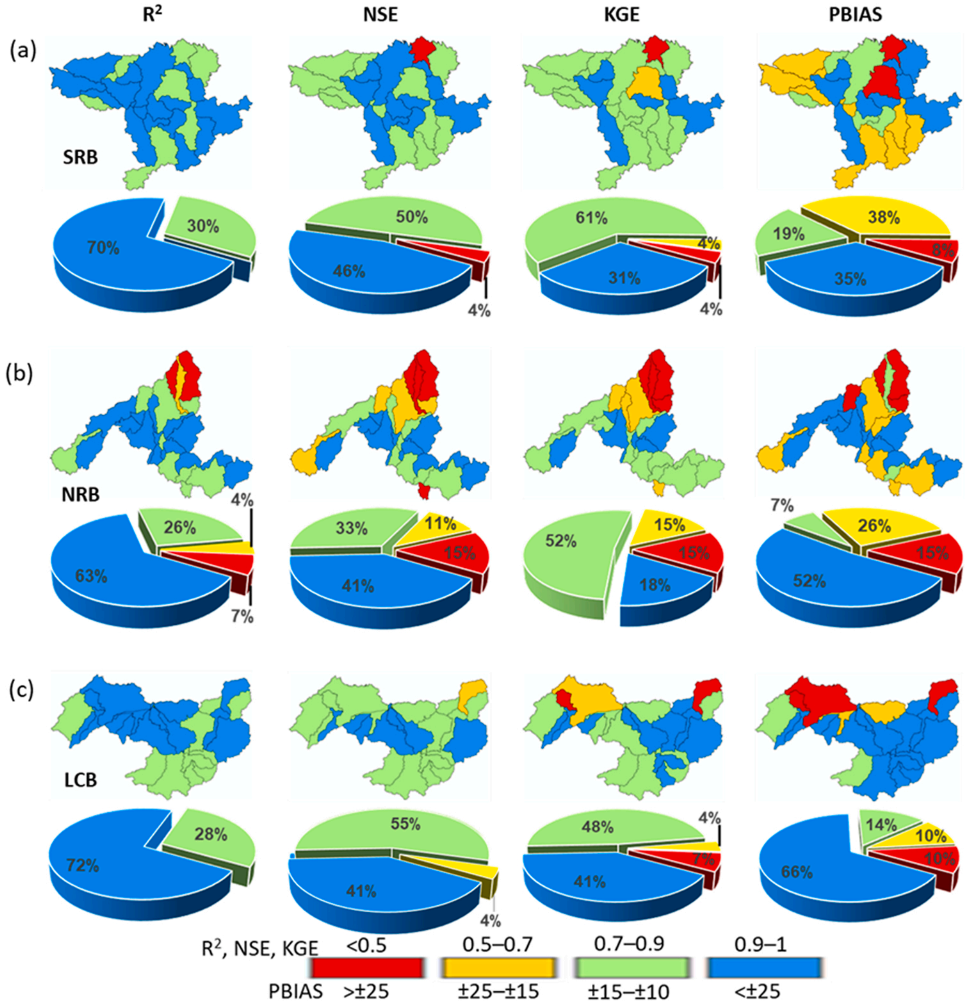

Fig. 3. Spatial distribution of performance metrics (R^2, NSE, KGE, and PBIAS) of calibration of the SWAT model using ETa of ETMonitor product for SRB (a), NRB (b), and LCB (c) from 2001 to 2010.

(3) Impacts of LULC change on WBCs

The quantification of impact of LULC change alone on the water balance components, we assumed that daily meteorological (and precipitation) conditions in the period of 2001–2010 and 2011–2020 were the same as that in 1990–2000 (frozen meteorological and precipitation conditions). We divided the period of 2001–2020 into two LULC scenarios: 2001–2010 as land-use scenario 1 (LUS1) by using LULC data of 2010, and 2011–2020 as land-use scenario 2 (LUS2) by using LULC data of 2020. The SWAT model was run for the entire period of 1990–2020 by taking the frozen meteorological (and precipitation) data in 1990–2000 and corresponding LULC data for the corresponding LULC data for each period. The impact of LULC change on a WBC in each LULC scenario period was calculated as:

$$\Delta WBC_{\mathrm{LUi}} = WBC_{\mathrm{LUSi}} - WBC_{\mathrm{BL}} \tag{7}$$

where $\Delta WBC_{\mathrm{LUi}}$ is the change in a water balance component between the corresponding period (LUS1 or LUS2) and the baseline period, WBC_{LUSi} is the value of a water balance component for either LUS1 or LUS2, WBC_{BL} is the value of a water balance component in the baseline period. This experiment (Eq. (7)) gave the results of impact by LULC change only during the two periods of 2001–2010 and 2011–2020.

3.2.2. Impact score of LULC change and climate variability on WBCs

The impacts of the changes in LULC and of climate variability on water balance components, i.e., ΔSURQ, ΔETa, ΔGW_RCH, ΔSW, ΔGWQ, and ΔWYLD, were estimated by Eqs. (6)–(7) for each LULC scenario (LUS1 and LUS2) and each climate scenario (CLS1 and CLS2) relative to the baseline. To identify which factor dominated the impact, we calculated the impact scores of LULC change and climate variability following the method by Nie et al. (2021):

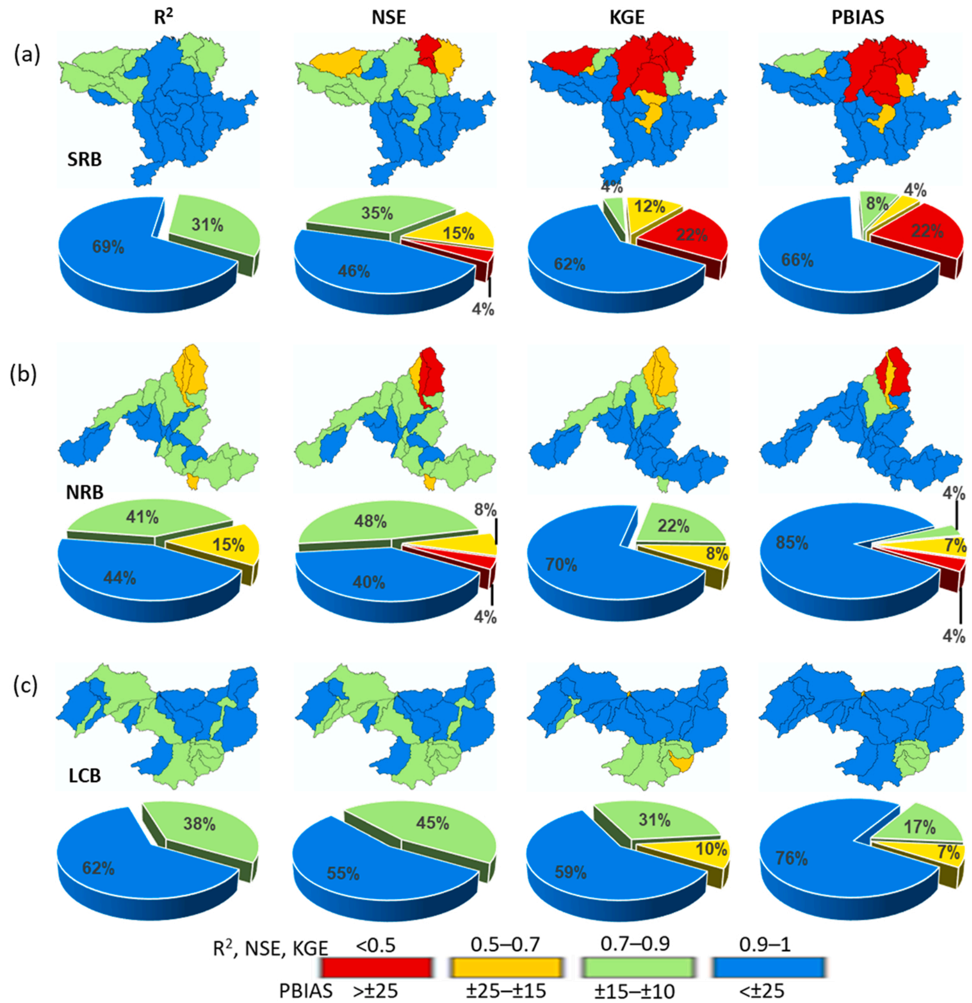

Fig. 4. Spatial distribution of performance metrics (R^2, NSE, KGE, and PBIAS) of validation of the simulated soil moisture by the calibrated SWAT model against NNsm-SM (a2, b2, and c2) for SRB (a), NRB (b), and LCB (c) from 2013 to 2020.

$$CR\_WBC_{CLi} = \Delta WBC_{CLi} / \Delta WBC \tag{8}$$

$$CR\_WBC_{LUi} = \Delta WBC_{LUi} / \Delta WBC \tag{9}$$

where CR_WBC_{CLi} and CR_WBC_{LUi} are the separate impact scores on water balance components, i.e. actual ET, SW, GW_RCH and SURQ, caused by climate variability and caused by LULC change, respectively;ΔWBC_{CLi} was calculated by Eq. (6);ΔWBC_{LU} was calculated by Eq. (7);ΔWBC is the change in a water balance component caused by the combined impact of LULC change and climate variability relative to baseline and calculated by Eq. (5). Higher scores (i.e., higher values of CR_WBC_{CL} or CR_WBC_{LU}) indicate higher impact.

4. Results

4.1. Results of SWAT calibration and validation

In the three basins, the calibration using monthly ETMonitor retrievals of actual ET indicated a good performance with values of R^2, NSE, and KGE greater than 0.7 and PBIAS values lower than ± 15% (Fig. 3). The validation for the three basins using monthly NNsm soil moisture (Fig. 4) showed that R^2, NSE, and KGE were higher than 0.7 and PBIAS lower than ± 15%. Moreover, this high performance of SWAT calibration was confirmed by comparing actual ET across the sub-basins of the three basins (Fig. A2, A3, and A4).

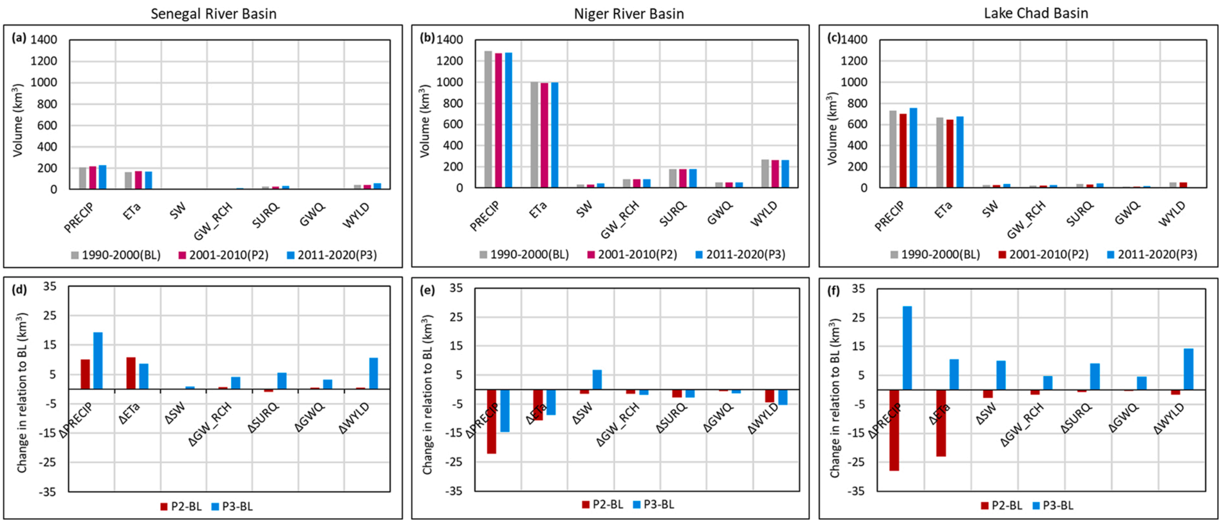

Fig. 5. Decadal average of annual WBCs in the three periods in SRB (a), NRB (b), and LCB (c), and the changes in WBCs caused by combined impacts of LULC and climate variability in P2 and P3 relative to the baseline period in SRB (d), NRB (e) and LCB (f).

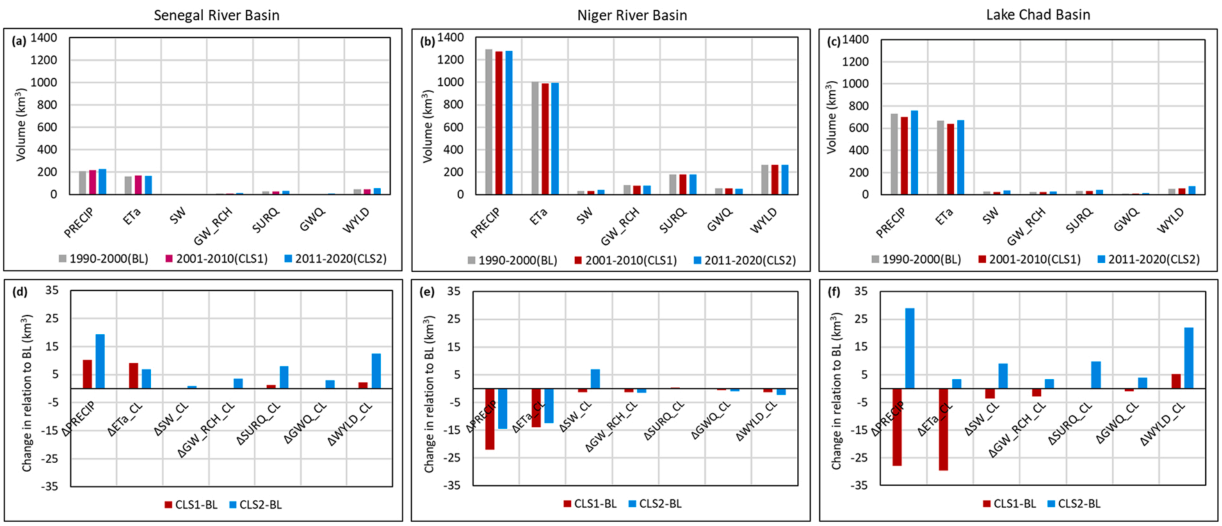

Fig. 6. Decadal average of annual WBCs in the three periods in SRB (a), NRB (b), and LCB (c), and the changes in WBCs caused only by climate variability in CLS1 and CLS2 relative to the baseline period in SRB (d), NRB (e) and LCB (f).

4.2. Impacts of LULC changes and climate variability on water balance components

4.2.1. Combined impacts

Fig. 5 displays the results on the combined impact of climate and LULC changes on ETa, SW, SURQ, GW_RCH, GWQ and WYLD in each of the three periods, i.e., 1990–2000 (P1 = BL) with LULC1990, 2001–2010 (P2) with LULC2010, and 2011–2020 (P3) with LULC2020 in the three basins of SRB, NRB and LCB. In P1, all WBCs decreased in NRB and LCB, while in contrary in SRB most WBCs increased except for surface runoff (Fig. 5d, e, f). In P3, all WBCs increased in SRB and LCB, while in NRB most WBCs decreased except for soil water content (SW).

4.2.2. Separation of impacts of LULC and climate variability

4.2.2.1. Impact assessment at basin level. The impacts of climate variability on ETa, SURQ, SW, GW_RCH, GWQ, and WYLD in the three watersheds during 2001–2010 were evaluated using climate 2001–2010 and during 2011–2020 using climate 2011–2020 with frozen LULC at LULC1990, named CLS1 and CLS2 respectively. These experiments were evaluated by taking the corresponding WBCs in the climate baseline period (i.e. climate 1990–2000 with LULC1990) (Fig. 6d, e and f) as a reference. The impacts of LULC change on ETa,

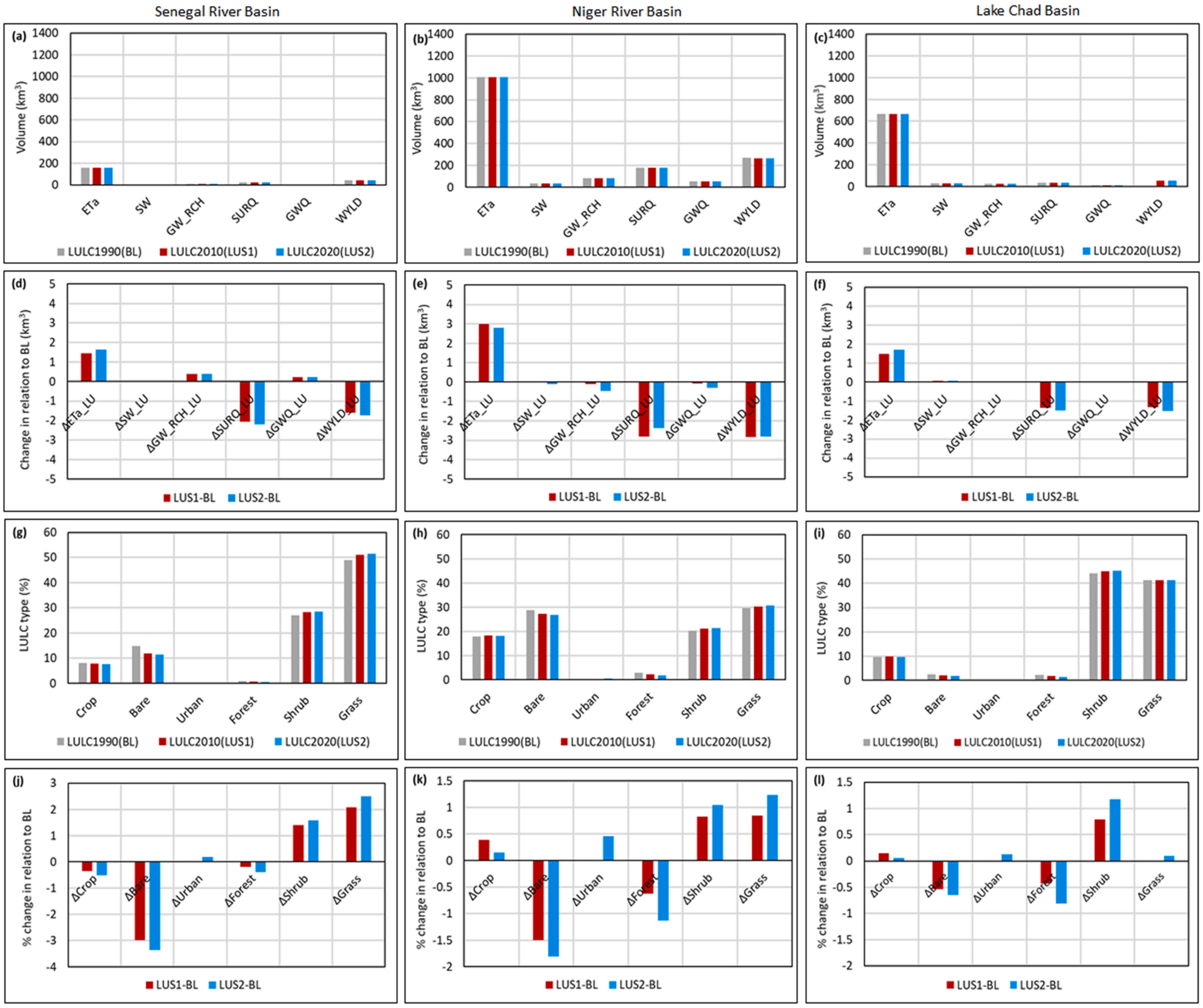

Fig. 7. Decadal average of annual WBCs in the three periods in SRB (a), NRB (b), and LCB (c), and the changes in WBCs caused only by LULC change in LUS1 and LUS2 relative to the baseline period in SRB (d), NRB (e) and LCB (f). (h, i, j) are the fractional abundance of LULC types in the scenarios of BL, LUS1 and LUS2, (k, l, m) are the changes in LULC types in LUS1 and LUS2 relative to BL in SRB, NRB and LCB.

Table 4
Summary of key findings of changes in water balance components caused by climate variability and LULC changes for the study period (2011–2020) compared to baseline period (1990–2000) for the basins of SRB, NRB and LCB (all variables are in km^3).

	Water loss		Groundwater recharge		Potential water recycling					
WBCs	Actual ET		GW_RCH		SURQ		GWQ		LATQ	
Basins/Factors	climate	LULC	climate	LULC	climate	LULC	climate	LULC	climate	LULC
SRB	7	1.6	3.6	0.4	8	-2	3	0.2	1.6	0.2
NRB	-12	3	-1.5	-0.5	0	-2	-1	-0.3	-1.4	-0.1
LCB	3.4	1.7	3.3	0	9.75	-1.5	4	0	0.9	0.01

Increase Decrease

SURQ, SW, GW_RCH, GWQ, and WYLD in the three watersheds during 2001–2010 using LULC2010 and 2011–2020 using LULC2020 with frozen climate at 1990–2000, i.e. LUS1 and LUS2 respectively, were evaluated by taking the corresponding WBCs in the climate baseline period (i.e. Climate 1990–2000 with LULC1990) (Fig. 7d, e and f) as a reference. Fig. 7g-i and j-l show the abundance of LULC

Table 5
Sum of annual precipitation and water yield (km^3/year) in each period in the three watersheds and the ratio of water in and water out. It is assumed that Q_TLOSS = 0 on annual basis.

Basin	Scenario	PREC = W_{in} (km^3)	SURQ (km^3)	GWQ (km^3)	LATQ (km^3)	WYLD = W_{out} (km^3)	R_{oiR} (km^3)
LCB	BL	728.82	35	11	6.5	52.5	0.07
	LUS1	728.82	33.68	10.95	6.49	51.12	0.07
	LUS2	728.82	33.53	10.93	6.50	50.96	0.07
SRB	BL	206.69	26.30	4.31	12.92	43.53	0.21
	LUS1	206.69	24.25	4.53	13.14	41.92	0.20
	LUS2	206.69	24.11	4.53	13.14	41.78	0.20
NRB	BL	1294.54	180.21	54.73	28.00	262.94	0.20
	LUS1	1294.54	177.41	54.65	28.04	260.10	0.20
	LUS2	1294.54	177.83	54.45	27.88	260.16	0.20

types and the changes in LULC types during the two LULC scenarios, named LUS1 and LUS2, respectively.

Senegal river basin. The assessment of climate variability impacts on WBCswais done as described in Section 3.2.1. (2), i.e. based on the changes in WBCs during CLS1 and CLS2 compared to the baseline climate. The precipitation (PRECIP) increased during both CLS1 and CLS2, i.e.,in the near and far post-drought periods compared to post-drought period, which led to a rise in all WBCs (Fig. 6d). Particularly, during the far post-drought period (i.e. CLS2), the rainfall increased by about 20 km^3, which led to a rise in fresh water availability and expanding water recycling within the basin by increasing surface runoff, groundwater return flow and lateral flow by 8 km^3, 3 km^3 and 1.6 km^3 respectively (Fig. 6d, Table 4). Moreover, a rise in groundwater recharge by 3 km^3 was estimated (Table 4). During the three periods, the dominant LULC classes were Shrub land, Grassland, bare land, cropland, and forest, respectively covering 30%, 50%, 10%, 7% and 2% of the watershed (Fig. 7g). Water bodies, wetland, and urban areas were minor LULC types (less than 0.5%) (Table A2). The assessment of LULC change impact on WBCs was done as described in Section 3.2.1. (3), based on the changes in WBCs during CLS1 and CLS2 compared to the baseline climate and LULC. The changes in LULC were a decrease in bare land, forest and cropland area and an expansion of grassland and shrub land (Fig. 7j). The expansion of natural vegetation in the three watersheds led to an increase in actual ET and a decline in freshwater availability due to the decrease in SURQ, GWQ and LATQ (Fig. 7d, Table4).

Niger river basin. The assessment of climate variability impact on WBCs was done as described in Section 3.2.1. (2) based on the changes in WBCs during CLS1 and CLS2 compared to baseline. The precipitation during CLS1 and CLS2 (near and far post-drought periods) compared to BL decreased with a resulting decrease in all water balance components (Fig. 6e). The continuation of the severe drought, i.e. the decrease in precipitation, clearly affected the freshwater availability and water recycling within the Niger river basin. The dominant LULC classes were Shrub land, Grassland, bare land, cropland, and forest, respectively covering 20%, 30%, 28%, 18% and 3% of the watershed (Fig. 7h). Water bodies, wetland, and urban areas were minor LULC types (less than 0.5%) (Table A3). The assessment of LULC change impact on WBCs was done as described in Section 3.2.1. (3), based on the changes in WBCs during LUS1 and LUS2 compared to the baseline scenario. The changes in LULC were characterized by a decrease in bare land and forest area and an expansion of grassland, shrub land, and cropland (Fig. 7k). The expansion of natural vegetation in the three watersheds led to an increase in actual ET and a decline in freshwater availability by decreasing surface runoff, lateral flow, and groundwater return flow (Fig. 7e, Table 4).

Lake Chad basin. The assessment of climate variability impact on WBCs was done as described in Section 3.2.1. (2), based on the changes in WBCs during CLS1 and CLS2 compared with the baseline climate. During the near post-drought period, a decrease in rainfall was estimated, which led to a decline in all water balance components compared to the post-drought period (BL). During the far post-drought period, the precipitation increase triggered a rise in all water balance components, particularly surface runoff, lateral flow, and return flow (Fig. 6f), i,e, an increase in freshwater availability and water recycling. The dominant LULC classes were Shrub land, Grassland, bare land, cropland, and forest, respectively covering 45%, 40%, 3%, 10% and 2% of the watershed (Fig. 7i). Water bodies, wetland, and urban areas were minor LULC types (less than 0.5%) (Table A4). The assessment of LULC change impact on WBCs was done as described in Section 3.2.1. (3), based on the changes in WBCs during LUS1 and LUS2 compared with the baseline climate and LULC. The changes in LULC were characterized by a decrease in bare land and forest area and an expansion of grassland, shrub land, and cropland (Fig. 7l). The expansion of natural vegetation in the three watersheds led to an increase in actual ET, with a decline in freshwater availability and potential water recycling by decreasing surface runoff, lateral flow and groundwater return flow (Fig. 7l, Table 4).

4.2.2.2. Water recycling assessment. The results on the Water Ratio in/out Recycling (R_{oiR}) index indicated that this index had a value of 0.2, 0.07 and 0.2 in SRB, LCB and NRB respectively (Table 5), which means that water yields from the watershed were about 20%, 7% and 20% of the precipitation in SRB, LCB and NRB respectively. Hence, an amount of water s transferred from sub-basins upstream to the next sub-basin downstream within the watershed, which we call water recycling. Thus, water recycling provides an additional volume of water which could be diverted for irrigation or to another reservoir from upstream to downstream. We did not explore it further for the reasons explained earlier (Set. 3.4).

4.2.2.3. Impact assessment by sub-basins. After we selected the hotspots in terms of LULC change, we analyzed the combined impacts of LULC change and climate variability on actual evapotranspiration, surface runoff, soil water, groundwater recharge, groundwater

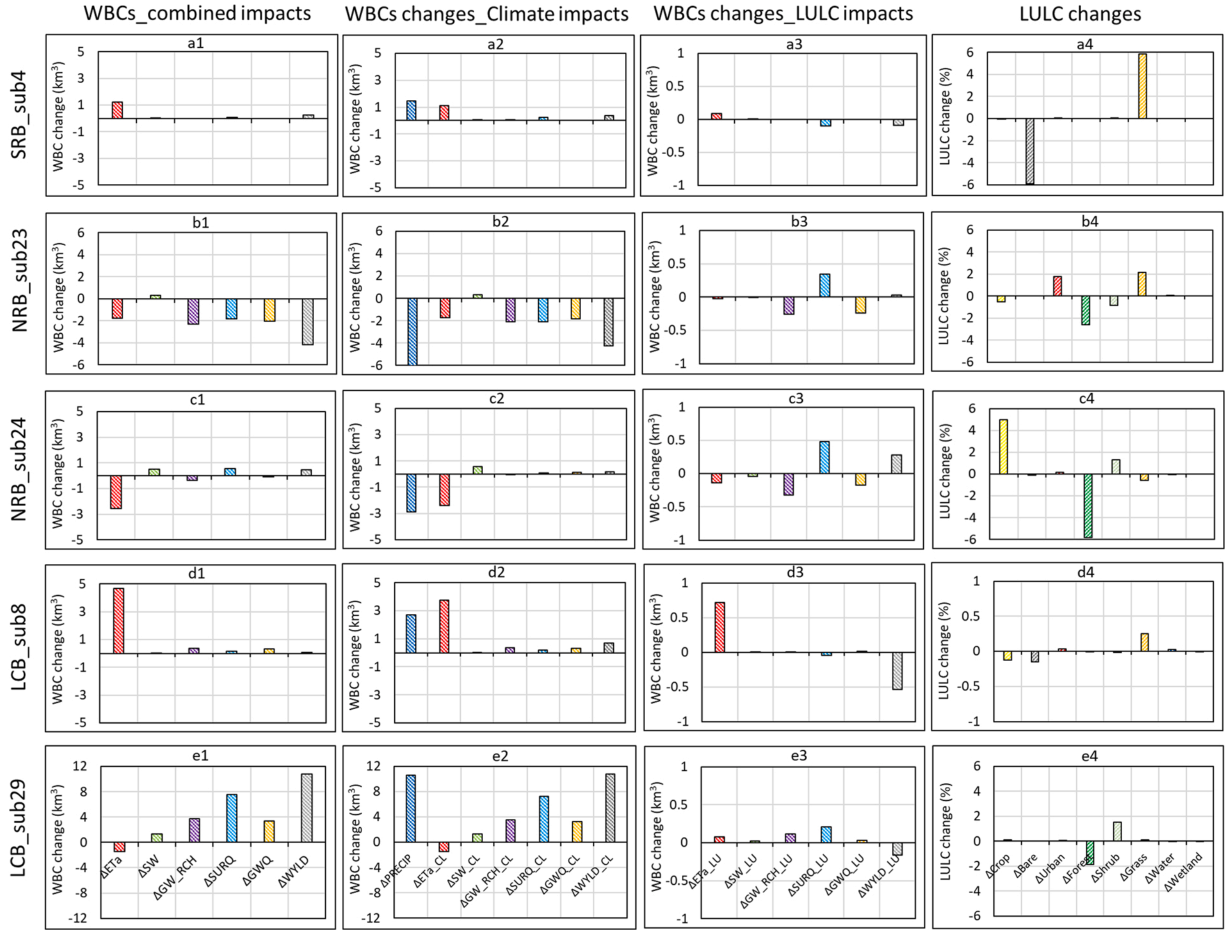

Fig. 8. Decadal average of annual change in actual evapotranspiration (ETa), soil water (SW), groundwater recharge (GW_RCH), surface runoff (SURQ) and water yield (WYLD) caused by the combined impact of LULC change and climate variability (column 1), caused only by climate variability (column 2), and caused only by LULC change (column 3) between LULC1990 with climate 1990–2000 and LULC2020 with climate 2011–2020 in SRB_sub4 (a1-a4), NRB_sub23 (b1-b4), NRB_sub24 (c1-c4), LCB_sub8 (d1-d4), and LCB_sub29 (e1-e4).

return flow, and water yield in response to these transitions. The average annual changes of water balance components in response to the change in LULC area between LULC1990 and LULC2020 and between climate 1990–2000 and 2011–2020 are shown in Fig. 8. The greatest positive change of actual evapotranspiration caused by the combined impact of LULC change and climate variability (4.7 km^3) was in sub-basin 8 of the Lake Chad basin (Fig. 8 d1). As regards the analysis of the separate impacts of LULC change and climate variability, the increase in ETa was mainly caused by climate variability (3.8 km^3), specifically the increase in precipitation (Fig. 8 d2), rather than the increase in natural vegetation (Fig. 8 d3). The most significant decline in surface runoff, groundwater recharge and groundwater return flow caused by the combined impact of climate variability and LULC change appeared in sub-basin 23 of Niger River basin (Fig. 8 b1). After investigating the separate impacts of LULC change and climate variability, we found that this decrease of three variables was mainly due to climate variability (Fig. 8 b2) rather than LULC change (Fig. 8 b3). The sub-basin 24 in NRB showed an increase in surface runoff (Fig. 8 c3), despite the rainfall deficit, due to the increase in cropland at the expense of forest (Fig. 8 c2 and c4). The highest increase in surface runoff, groundwater recharge, and groundwater return flow caused by climate variability and LULC change was in sub-basin 29 of Lake Chad basin (Fig. 8 e1). After examining the separate impacts of the two drivers, we figured out that this increment in surface runoff, groundwater recharge, and groundwater return flow was triggered by climate variability (Fig. 8 e2).

4.2.3. The contribution of specific LULC types to the impact of LULC change

Overall, the results (Fig. 9) indicated that the re-greening of the study area, caused by the increase of grassland and shrub land at the expense of bare land and forest loss, led to an increase in actual ET, which triggered a decrease in SURQ. In the Senegal River (Fig. 9 a1 and a2) and Niger River basins (Fig. 9 b1 and b2), both LUS1 and LUS2 are characterized by an important gain of grassland and shrub land at the expense of bare land. This gain triggered a rise in actual ET and a decrease in SURQ, accompanied by an increase in GW_RCH and SW (Fig. 9 a3 and a4). The Niger River basin showed a gain in cropland which led to reduce the decline of SURQ. The increase in shrub land area led to a rise in GW_RCH and SW, but it was smaller than the decline caused by forest loss. On the contrary, a

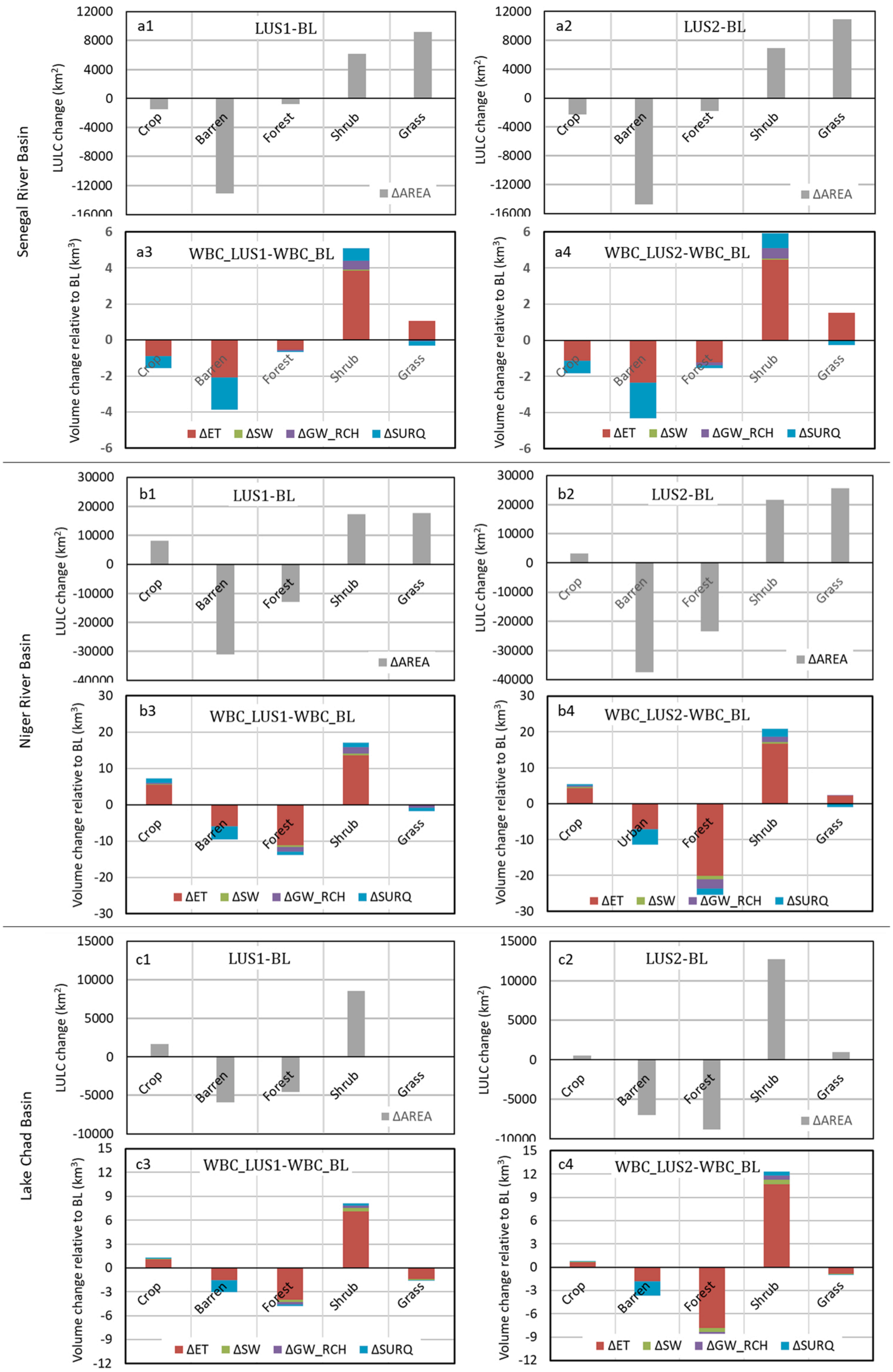

Fig. 9. Changes in major LULC types in LUS1 and LUS2 compared to BL in (a1, a2) SRB, (b1, b2) NRB and (c1, c2) LCB; changes in ETa, SW, GW_RCH, and SURQ generated by each LULC class for LUS1 and LUS2 relatively to BL in (a3, a4) SRB, (b3, b4) NRB, and (c3, c4) LCB.

noticeable gain in the grassland area was detected, but the grassland actual ET increased slightly (Fig. 9 b3 and b4). In the Lake Chad basin (Fig. 9 c1 and c2), an expansion in shrub land and cropland areas at the expense of bare land was identified, causing an increase in actual ET and a decline in SURQ. At the same time, the reduction in forest triggered a decrease in GW_RCH and SW (Fig. 9 c3 and c4). A meager increase in grassland (about 100 km^2) was estimated, while the actual ET decreased due to the shifting of grassland from the

Table 6
Change in the percentage contribution of LULC types to WYLD.

LULC	Percentage contribution of each LULC type to water yield (%)					
	SRB		NRB		LCB	
	BL	LUS2	BL	LUS2	BL	LUS2
Crop	17.51	15.19	32.36	32	17.85	19.48
Bare	12.42	9.94	6.38	5.72	36.35	28.41
Forest	36.77	41.67	25.68	27.99	24.21	28.63
Shrub	26.42	26.72	27.03	26.28	16.10	17.54
Grass	6.85	6.45	8.52	7.99	5.49	5.93
LULC	Change in LULC area and percentage contribution					
	SRB		NRB		LCB	
	area change (km^2)	contribution change (%)	area change (km^2)	contribution change (%)	area change (km^2)	contribution change (%)
	LUS2-BL	LUS2-BL	LUS2-BL	LUS2-BL	LUS2-BL	LUS2-BL
Crop	-2220	-2.33	3181	-0.36	553	1.63
Bare	-14737	-2.48	-37461	-0.65	-7002	-7.94
Forest	-1745	4.90	-23405	2.30	-8789	4.42
Shrub	6909	0.30	21589	-0.74	12756	1.44
Grass	10940	-0.40	25570	-0.53	1001	0.44

Table 7
The impact scores of LULC change (CR_LU) and climate variability (CR_CL) on WBCs in the P2 (2001–2010) and P3 (2011–2020) for the basins of SRB, NRB and LCB in the Sahel. Numbers in bold indicates the dominant impacts.

Basin	Period	CR	Actual ET	SW	GW_RCH	SURQ
SRB	P1	CR_CL	**0.85**	**1.15**	0.40	-1.53
		CR_LU	0.13	-0.21	**0.57**	**2.35**
	P2	CR_CL	0.79	**0.96**	**0.87**	**1.45**
		CR_LU	0.19	0.04	0.09	-0.40
NRB	P1	CR_CL	**1.32**	**0.95**	**1.01**	-0.09
		CR_LU	-0.29	0.00	0.06	**1.01**
	P2	CR_CL	**1.43**	**1.02**	**0.82**	0.02
		CR_LU	-0.32	-0.01	0.24	**0.86**
LCB	P1	CR_CL	**1.05**	**0.99**	**0.94**	-0.64
		CR_LU	-0.06	-0.02	-0.01	**1.78**
	P2	CR_CL	**0.83**	**0.97**	**0.98**	**1.15**
		CR_LU	0.16	0.01	0.00	-0.16

humid to arid part of the watershed (Barnieh et al., 2022). Human contribution plays an important role in the evolution of Sahel region's hydrological response. The water balance variation, however, was mostly impacted by the re-greening of the Sahel through the expansion of shrub land and grassland at the expense of bare land and forest. The man-made LULC changes had a crucial contribution to the increase of actual ET and SURQ, mainly by the expansion of cropland in the Niger River and Lake Chad basins.

Furthermore, we have calculated the percentage contribution of the water yield by each major LULC type to the total WYLD of all major LULC classes. Then we investigated the change in the percentage contribution from 1990 to 2020 to identify the LULC types which highly reduced water yield (Table 6).

In SRB the WYLD decreases was related to the loss in bare land and crop land. The decrease in forest had a positive impact on WYLD. In NRB the increase in shrub land and grassland at the expense of bare land led to a decrease in WYLD. Furthermore, the increase in crop land had a negative impact on WYLD. Contrariwise, forest loss had a positive impact on WYLD. In LCB, mainly the conversion of bare land to shrub land and grassland had a major impact on WYLD decline.

4.2.4. Impacts of LULC changes vs. climate variability

The impact scores (CR) of the LULC change (CR_LU) and climate variability (CR_CL) on each water balance component, i.e. ETa, SURQ, GW_RCH and SW, were calculated for P2 (2001–2010) and P3 (2011–2020) according to the procedure described in Section 3.2.2 (Eqs. (8) and (9)), and given in Table 7. An absolute value of CR_LU of a variable close or higher than 1 means that variable is impacted by a LULC change. If the absolute value of CR_CL of the variable is close or higher than 1, it means the variable is impacted by climate variability.

In the Senegal River basin, during P2, climate variability was the dominant driver in increasing the actual ET with CR_CL 0.85 and decreasing SW (CR_CL=1.15). At the same time, the LULC change was the main driver of increasing GW_RCH with CR_CL about 0.57. The combined LULC change and climate variability decreased SURQ, mainly due to the impact of LULC changes, which led to its decrease with CR_LU about 2.3. In contrast, climate variability contributed to the increase in SURQ with CR_CL = -1.5, , i.e., lower and opposite sign than the impact of LULC change. During P3, climate variability was the dominant driver of the rises in ETa, SW, GW_RCH, and SURQ with CR_CL values of 0.79, 0.96, 0.87, and 1.45 respectively, scores of CR_LU are much smaller.

In the Niger River basin, the ETa, GW_RCH, and SW were highly impacted by climate variability, with CR_CL equal to 1.32, 0.95, and 1.01, respectively, during P2, and 1.43, 1.02, and 0.82, respectively, during P3. In both periods, the SURQ which was decreasing during both P2 and P3, was impacted mainly by the LULC changes with CR_LU values equal to 1.01 and 0.82, respectively.

In Lake Chad Basin, the actual ET, SW and GW_RCH were highly affected by climate variability, with CR_CL equal to 1.05, 0.99, and 0.94 respectively during P2 and 0.83, 0.97, and 0.98 respectively during P3. The SURQ was decreasing during P2 and it was mainly influenced by LULC changes with CR_LU equal to 1.78 while during P3 SURQ was increasing and it was influenced by climate variability with CR_CL equal to 1.15.

5. Discussion

5.1. Calibration and validation performance

According to Moriasi et al., (2007, 2015), and Kouchi et al. (2017), the PBIAS values indicate the goodness of the model performance. In our study, the calibration of the SWAT model in the three watersheds using remote sensing actual ET from ETMonitor (ETMonitor_ETa) at monthly time steps gave PBIAS values $\leq \pm$ 15%. The PBIAS values in this study were lower than those found in the study by Odusanya et al. (2019) in the Ogun River Basin in Nigeria using actual ET from MOD16 (MOD16_ETa) and GLEAM (GLEAM_ETa). The outcomes of our study were also confirmed by Poméon et al. (2018) when they used MOD16 for SWAT model validation in West Africa. Furthermore, our results agreed with Lopez et al. (2017) findings in Morocco. The validation results in our work were also confirmed by Poméon et al. (2018) and Odusanya et al. (2019) when they calibrated and validated the SWAT model using remote sensing soil moisture. They reported that the dynamic of the SWAT_SM fit very well with the remote sensing SM retrievals (ESA CCI SSM (%)) in the upper few centimeters of the soil profile in most of the basin at a monthly time step.

5.2. Comparison with previous studies

We compared our results with previous studies (Table A5). The huge difference between the results of the first two studies by Sane et al. (2020) in the upper reach of the Senegal River Basin (SRB) is due to the difference in study areas and periods. The three other studies simulated the surface runoff (SURQ) in different sub-catchments of SRB during recent periods. The results of the two studies carried out by Faty et al. (2019) and Sun et al. (2013) showed comparable surface runoff values with our study. Furthermore, the above mentioned three studies were carried out in small catchments in SRB, while in our study the SURQ was estimated for the whole SRB. The first two studies (numbers 9 and 10 in Table A5) in the Niger River Basin (NRB) showed SURQ values lower than that in our study (Andersen et al., 2012; Descroix et al., 2009). These two studies were carried out in two small catchments in the NRB, while our study was done for the whole NRB. Therefore, it might be concluded that these difference in the simulated SURQ between our study and other studies in smaller areas was partly due to the difference in spatial coverage. Moreover, the study by Mamadou et al. (2015) in the small Koris basin (in NRB) showed comparable results to ours. Likewise, in the Lake Chad Basin (LCB), almost all studies in previous work were done in the Chari-Logone basin, whereas our study was carried out for the entire southern LCB. Studies numbered 16–19 in Table A5 (Descroix et al., 2009; Lemoalle et al., 2012; Mahamat Nour et al., 2021; Zhu et al., 2017) showed comparable results to our study. Furthermore, the majority of the studies in the three watersheds have different spatial and temporal coverage, which leads to some differences compared to our findings. However, the surface runoff simulated in our study is comparable to recent studies in different catchments.

5.3. Assessment of combined and separate impacts of LULC changes and climate variability

In SRB, the decrease in SURQ during period 2 (P2 = 2001–2010) compared to the baseline (P1 = BL=1990–2000) due to the dominant impact of natural vegetation expansion in decreasing SURQ. This outcome agrees with the findings of Diop et al. (2017), who reported a decrease in the upper reach of SRB. While the increase in SURQ during and period 3 (P3 = 2011–2020) compared to the baseline (P1 = BL=1990–2000) is explained by the dominant impacts of climate variability in increasing SURQ. This finding is confirmed by Wilcox et al. (2018). The increase in groundwater recharge (GW_RCH) was also detected by other studies, which did not provide estimates of groundwater recharge which led to a rise in return flow (Hollis, 1990). In LCB, The decrease in SURQ during P2, compared to the baseline, can be explained by the combined impacts of LULC changes and climate variability, as also confirmed by Mahmood and Jia (2019). On the other hand, SURQ increased during P3 compared with the baseline, similar results was reported by Pham-Duc et al. (2020). The latter study also underscored the contribution of groundwater to the recovery of the open water area of the LCB. Still, they did not mention or quantify the role of water recycling. In the NRB, the estimated decrease in SURQ and GW_RCH during both P2 and P3 does not agree with the findings of Boulain et al. (2009) and Favreau et al. (2009), i.e., that both SURQ and GW_RCH increased despite a rainfall deficit in two small catchments in NRB during the post-drought period.

In the SRB, the rise in SURQ, GW_RCH, and return flow (GWQ), during both CLS1 (2001–2010) and CLS2 (2011–2020) compared to baseline (1990–2000), was caused by the increase in rainfall. These findings of our study agree with Oyebande and Odunuga (2010). On the other hand, in the NRB, the decline in SURQ, GW_RCH, and GWQ caused by the deficit in rainfall during both CLS1 and CLS2 does not agree with the findings of Descroix et al. (2013), although they documented the decrease in actual ET due to the decline of rainfall. However, in some small catchments in the NRB, Descroix et al. (2018) reported a reduction of SURQ due to the rainfall deficit. In LCB, the decline in SURQ during CLS1 was clearly caused by rainfall deficit, as also confirmed by Mahmood and Jia (2019). Furthermore, our outcomes of increase in GW_RCH, GWQ and SURQ during CLS2 agreed with the study by Pham-Duc et al. (2020).

The decline in SURQ was due to the increase in actual ET, triggered by the gain in natural vegetation (vegetation recovery) at the

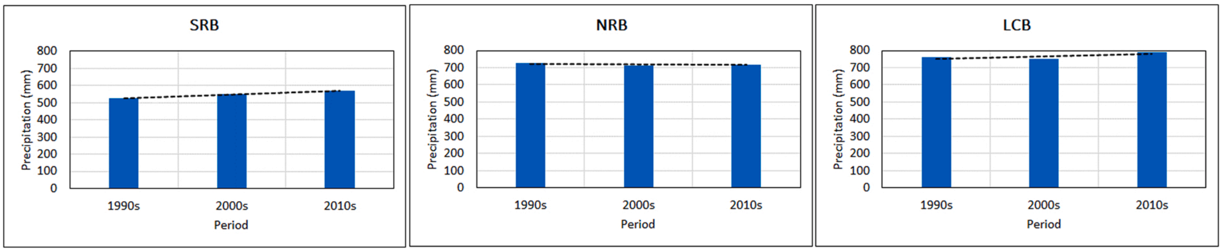

Fig. A.1. Precipitation during 1990 s, 2000 s, and 2010 s in the three basins SRB, NRB and LCB.

expense of bare land and forest loss during both LUS1 (LULC2010) and LUS2 (LULC2020), compared to baseline (LULC1990). This evidence emerged in the three watersheds. Similar result was also reported by Faty et al. (2019), particularly in the upper reach of SRB. This decrease in SURQ was also noted by Mahmood and Jia (2019) in the LCB. However, Boulain et al. (2009) and Favreau et al. (2009) reported an increase in SURQ and GW_RCH in the NRB, which disagrees with our findings. Our findings on a decrease in SURQ due to LULC change in NRB agreed with Daramola et al. (2022). The decrease in SURQ was more noticeable in SRB compared to NRB and LCB. This is probably due to the loss of cropland in SRB, while the crop area increased in NRB and LCB. These results suggest that an increase in cropland may trigger an increase in SURQ, as also found by several studies (Guzha et al., 2018; Lørup et al., 1998; Mao and Cherkauer, 2009; Op de Hipt et al., 2019), also in agreement with Aich et al. (2015) and Descroix et al. (2009). According to Giertz et al. (2005) this increase in surface runoff caused by cropland expansion could be explained by the decrease of macroporosity caused by the reduction of biological activity as a result of the disturbance of the soil by agricultural activities. The surface runoff increase is also probably due to the decrease in interception caused by land clearing and tree removal, which leads to a decrease in canopy interception. Further studies could be carried out by using satellite observation based data product (e.g. (Zheng and Jia, 2020), among others) to analyzing the impact of LULC change on the in canopy rainfall interception, thereafter on WBCs. In addition, the conversion from forest to cropland after land clearance reduces direct evaporation, which increases surface runoff (Leblanc et al., 2008; Mounirou et al., 2020). The results of this study on the decrease in surface runoff due to natural vegetation expansion disagreed with Trichon et al. (2018) and Descroix et al. (2018), who reported that the re-greening of the Sahel did not reduce the SURQ. At the same time, this gain in cropland was accompanied by a spread of natural vegetation at the expense of bare land loss, which led to an increase in actual ET in the same catchment (Ogutu et al., 2021). The water yield decreased in response to such LULC change, specifically the decline in SURQ was larger than the increase in GWQ and LATQ in SRB. On the other hand, the decrease in SURQ led to a decline in water yield in LCB.

The decline in potential water recycling as consequence of LULC change was mainly due to the vegetation recovery at the expense of bare land loss. The expansion of cropland in the Niger river basin had also a negative impact on water yield, while the deforestation had a positive impact on water yield in the three watersheds.

The re-greening of the region by expansion of grassland and shrub land led to an increase in actual ET and to a decrease in SURQ, as confirmed by Yonaba et al. (2021) and Ogutu et al. (2021). This vegetation recovery played a major role in increasing GW_RCH and soil water content (SW), and these results agreed with Marshall et al. (2012). This finding applied to three watersheds, but the change was larger in NRB and LCB than that in SRB, and in agreement with Mahmood and Jia (2019). Both climate variability and LULC change had nearly similar impacts on the hydrological response in the SRB. The LCB was more sensitive to the LULC change during P2. This process significantly reduced water availability by decreasing the SURQ and increasing the water loss via evapotranspiration, because of the higher actual ET. In contrast, climate variability was the main driver of increasing SURQ during P3, as also reported by Pham-Duc et al. (2020). The NRB was essentially impacted by climate variability.

Our study did not mean to say that our approach in general and independently from site-specific knowledge might be directly used by water managers, rather that it could be applied to understand better the hydrology in large and complex basins. Even more specifically, our study shows how LULC affects hydrological processes across a range of scales and basins with different hydrological characteristics and climate variabilities, and therefore how land management could aim at modifying water flows.

6. Conclusions

The assessment of the combined impacts of changes in LULC change and climate variability revealed that during the near post-drought period (2001–2010), the water balance components—both the absolute magnitude of water balance components and their relative fractions in the three watersheds—were rather different than that in the post-drought period (1990–2000, also as baseline period). In the far post-drought period (2011–2020), our findings indicated an increase in water balance components compared to the post-drought period in Senegal river and lake Chad basins and a decrease in the Niger river basin. These changes triggered a shortage of freshwater availability and showed that the first Sahelian hydrological paradox (see Introduction), i.e., a rise in surface water runoff despite the decline of precipitation, did not apply to Niger river basin. Furthermore, our findings indicated that the second hydrological paradox (see Introduction), i.e. a continuous increase in surface runoff despite the re-greening of the Sahel, did not apply to our study period and regions. During the far post-drought period, an increase in rainfall was estimated in both the SRB and the LCB, leading to a rise in freshwater availability and water recycling because of the increase in water yield. In the NRB, the shortage of water supply continued, resulting in the continuation of the drought in the basin, which showed that the Sahelian hydrological paradoxes described

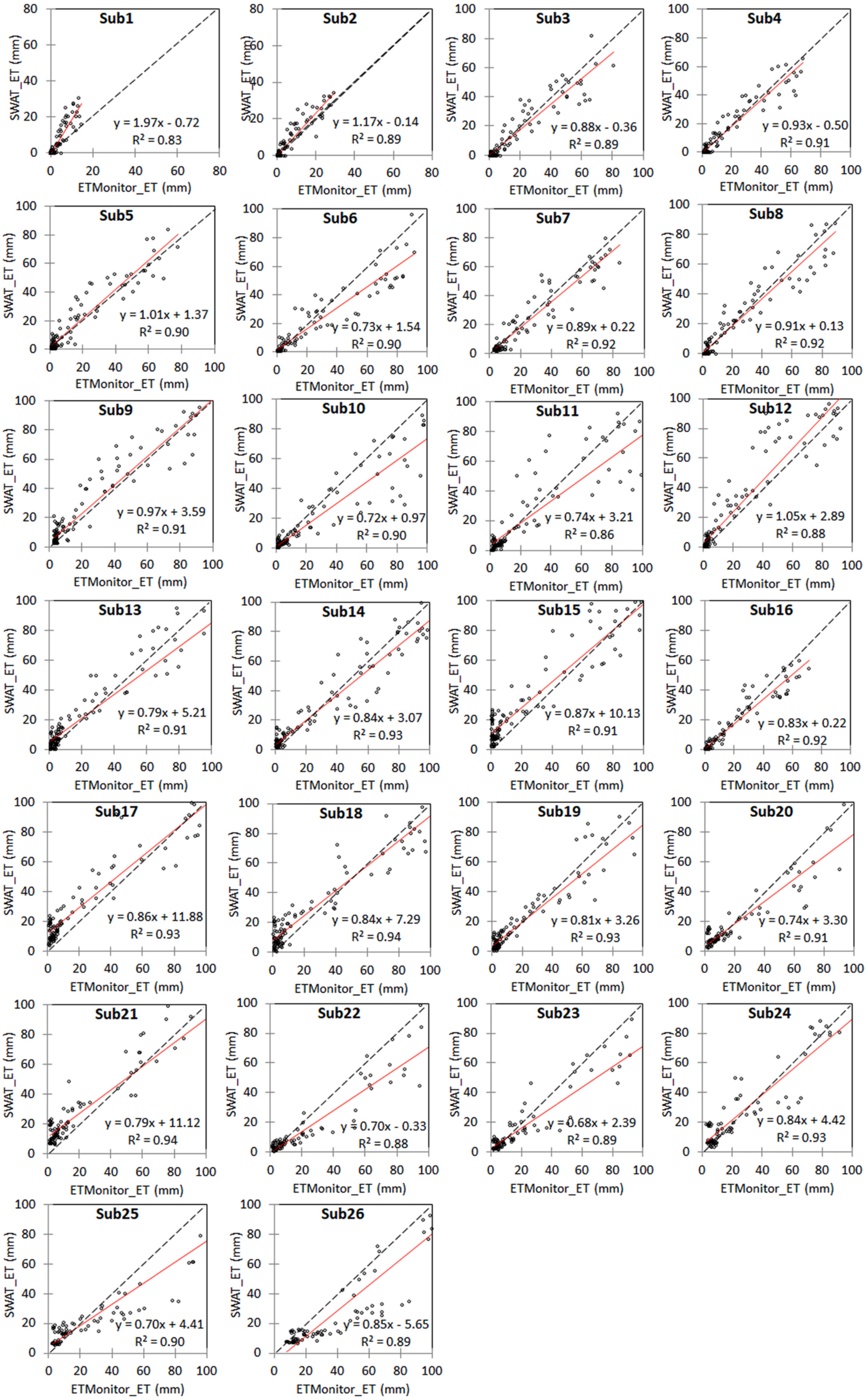

Fig. A.2. Comparison between ETM–ETa and SWAT–ETa for all sub-catchments in the SRB.

in the Introduction did not apply at basin level. These findings confirmed the rejection of the hypothesis (paradox), that is Sahel re-greening did not decrease surface runoff. In LCB and SRB, the increase in water yield, caused by climate variability, played an important role in improving water availability in the basin. Furthermore, the man-made extension of cropland at the expense of the forest loss had an important role in mitigating the decrease in surface runoff. Moreover, the continuous population growth led to an

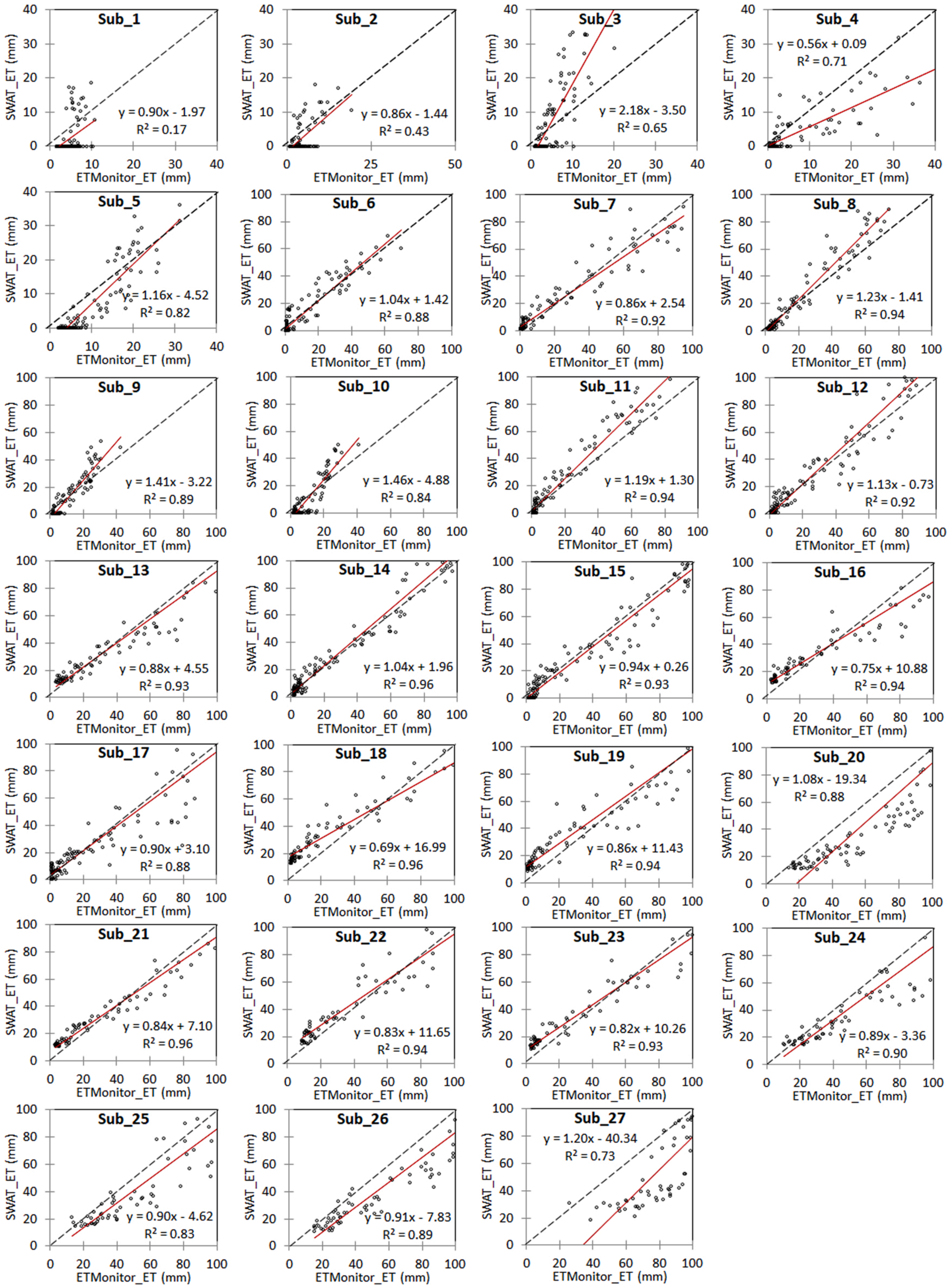

Fig. A.3. Comparison between ETM–ETa and SWAT–ETa for all sub-catchments in the NRB.

increase in the cultivated area at the expense of forest loss, i.e., a further increase in surface runoff. The latter may contribute to water recycling through water transfer from a sub-basin upstream to the next sub-basin downstream. These findings emphasized the crucial role of water recycling within the watershed, as well as gave a good hydrological insight into the interrelation of water and land management in the study area. The LULC change was the major responsible driver for the decrease in surface runoff and water yield,

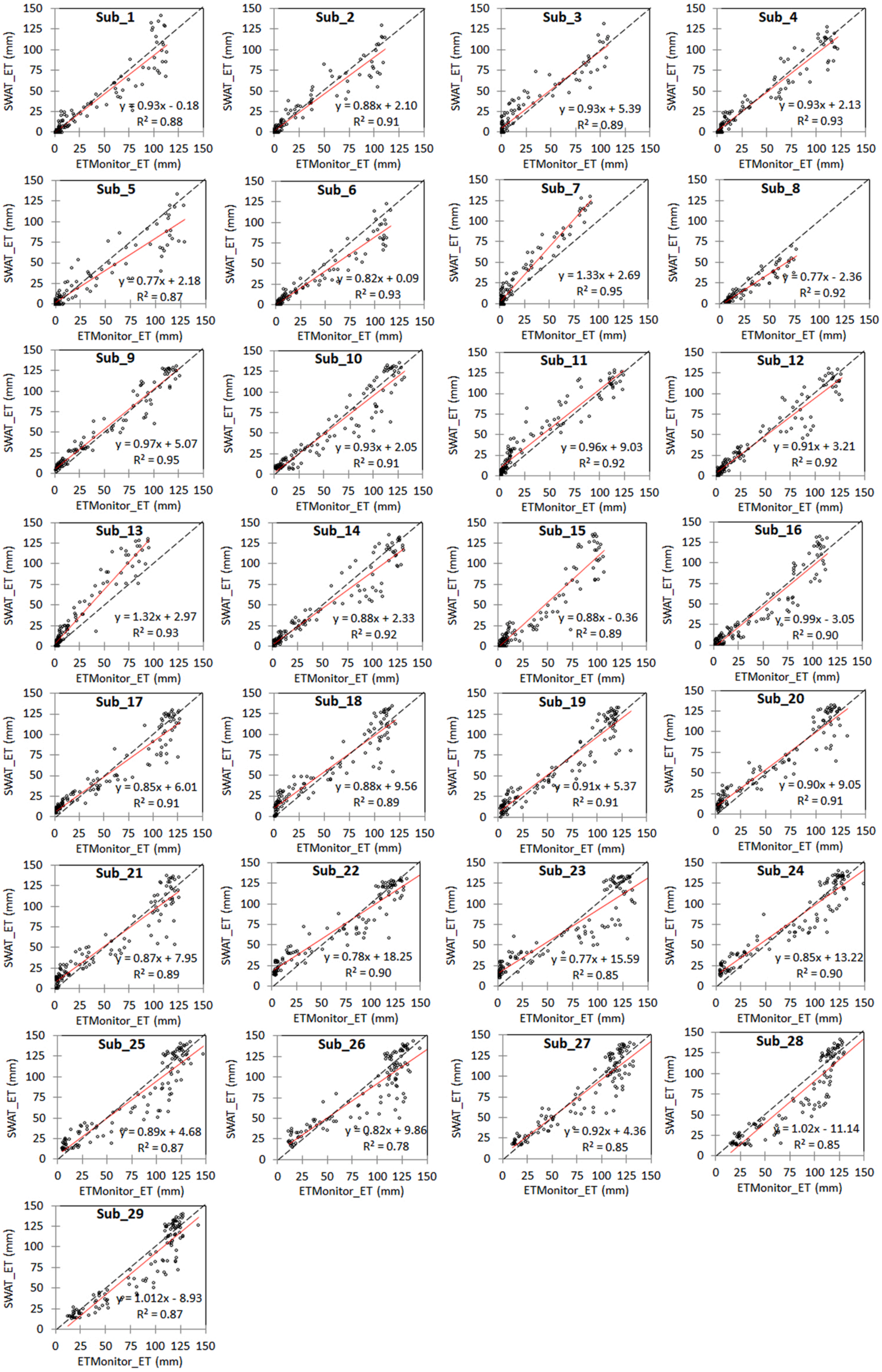

Fig. A.4. Comparison between ETM–ETa and SWAT–ETa for all sub-catchments in the LCB.

especially in the NRB during both the near post-drought (CR_LU=1) and far post-drought (CR_LU=0.85) periods, and in the LCB during the far post-drought (CR_LU=1.8) period. Thus, investigating the relationship between hydrologic response and LULC change in river basins at various spatial scales can help identify vulnerable sub-basins due to LULC changes. This could help prioritize effective land management practices to preserve sustainable water management.

Table A.1
List of abbreviations used in this study.

Abbreviation	Full name
Actual ET, ETa	Actual evapotranspiration
BL	Base line
CLS	Climate scenario
CR	Individual contribution rate
GWQ	Groundwater return flow
GW_RCH	Groundwater recharge
LATQ	Lateral flow
LCB	Lake Chad basin
LULC	Land use/land cover
LUS	Land use land cover scenario
NNsm	Neural network soil moisture
NRB	Niger River basin
PRECIP	Precipitation
R_{oiR}	Ratio water in/water out Recycling
SRB	Senegal River basin
SSM	Surface soil moisture
Sub	Sub-basin
SURQ	Surface runoff
SW	Soil water
SWAT	Soil and water assessment tool
WBC	Water balance components
W_{in}	Water in
W_{out}	Water out
WYLD	Water yield
ΔETa	Change in Actual evapotranspiration
ΔGWQ	Change in Groundwater return flow
ΔGW_RCH	Change in Groundwater recharge
ΔPRECIP	Change in precipitation
ΔSURQ	Change in Surface runoff
ΔSW	Change in Soil water
ΔWBC	Change in Water balance components
ΔWYLD	Change in Water yield

Table A.2
Different LULC types in the SRB.

		Senegal River Basin							
		AGRR	BARR	URBN	FRST	RNGB	RNGE	WATR	WETN
1990	km^2	35775	65111	6	3683	118244	214238	1299	51
	%	8.160	14.852	0.001	0.840	26.971	48.867	0.296	0.012
2010	km^2	34277	52016	31	2893	124418	223398	1321	55
	%	7.81	11.86	0.0069	0.65	28.37	50.95	0.30	0.0124
2020	km^2	33555	50373	794	1938	125153	225179	1357	58
	%	7.654	11.490	0.181	0.442	28.547	51.363	0.310	0.013
2010–1990	km^2	-1498	-13095	24	-790	6174	9159	22	3
	%	-0.342	-2.987	0.006	-0.180	1.408	2.089	0.005	0.001
2020–1990	km^2	-2221	-14737	788	-1745	6910	10941	59	7
	%	-0.507	-3.362	0.180	-0.398	1.576	2.496	0.013	0.002

Table A.3
Different LULC types in the NRB.

		AGRR	BARR	URBN	FRST	RNGB	RNGE	WATR	WETN
1990	km^2	373046	595431	459	59376	420767	612305	7982	1237
	%	18.02	28.76	0.02	2.87	20.32	29.57	0.39	0.06
2010	km^2	381224	564375	1143	46454	438007	629934	8324	1141
	%	18.41	27.26	0.06	2.24	21.15	30.42	0.40	0.06
2020	km^2	376228	557969	9994	35970	442357	637876	9044	1165
	%	18.17	26.95	0.48	1.74	21.36	30.81	0.44	0.06
2010–1990	km^2	8177	-31056	684	-12922	17240	17628	341	-95
	%	0.395	-1.500	0.033	-0.624	0.833	0.851	0.016	-0.005
2020–1990	km^2	3181	-37461	9536	-23406	21590	25571	1061	-72
	%	0.154	-1.809	0.461	-1.130	1.043	1.235	0.051	-0.003

Table A.4
Different LULC types in the LCB.

		AGRR	BARR	URBN	FRST	RNGB	RNGE	WATR	WETN
1990	km^2	104149	26695	277	23138	476836	445652	3839	121
	%	9.637	2.470	0.026	2.141	44.123	41.237	0.355	0.011
2010	km^2	105775	20826	361	18552	485381	445751	3968	91
	%	9.788	1.927	0.033	1.717	44.913	41.246	0.367	0.008
2020	km^2	104702	19692	1650	14349	489593	446653	3991	75
	%	9.688	1.822	0.153	1.328	45.303	41.330	0.369	0.007
2010–1990	km^2	1626.26	-5868.93	84.13	-4585.96	8544.43	99.41	129.14	-29.72
	%	0.150	-0.543	0.008	-0.424	0.791	0.009	0.012	-0.003
2020–1990	km^2	554	-7003	1373	-8790	12757	1002	153	-46
	%	0.051	-0.648	0.127	-0.813	1.180	0.093	0.014	-0.004

AGRR: Agriculture, BARR: Bare land, URBN: Urban area, FRST: Forest, RNGB: Shrub land, RNGE: Grass land, WATR: Water bodies, WETN: Wet land.

Table A.5
Comparison of water budget estimated in SRB, NRB, and LCB in different studies.

Basin	Number	Study	Study area	Time period	Mean runoff (mm)
SRB	1	Sane et al. (Sane et al., 2020)	Bafing River (upstream of SRB)	1979–1986	228
	2	Sane et al. (Sane et al., 2020)	Bafing River (upstream of SRB)	1988–1994	234
	3	Faty et al. (Faty et al., 2019)	Upper SRB	1968–2011	31.36
	4	Faty et al. (Faty et al., 2019)	Upper SRB	2011–2014	61.35
	5	Sun et al. (Sun et al., 2013)	Watershed of Bakel in SRB	1988–2008	48.66
	6	Our study	Senegal River Basin	1990–2000	60
	7	Our study	Senegal River Basin	2001–2010	58
	8	Our study	Senegal River Basin	2011–2020	72
NRB	9	World bank (Andersen et al., 2012)	Niamey in NRB	1980–2004	42
	10	Descroix et al. (Descroix et al., 2009)	Bani in NRB	1991–2000	54.1
	11	Mamadou et al. (Mamadou et al., 2015)	Small Koris in NRB	1998–2011	72.98
	12	Mamadou et al. (Mamadou et al., 2015)	Small Koris in NRB	2001–2010	81.12
	13	Our study	Niger River Basin	1990–2000	87
	14	Our study	Niger River Basin	2001–2010	85.7
	15	Our study	Niger River Basin	2011–2020	85.7
LCB	16	Descroix et al., (Descroix et al., 2009)	Chari river (LCB)	1991–2000	57.51
	17	Zhu et al. (Zhu et al., 2017)	Southern Pool of Lake Chad	1991–2013	40.52
	18	Mahamat Nour et al. (Mahamat Nour et al., 2021)	Chari–logone Basin	1960–2015	42
	19	Lemoalle et al. (Lemoalle et al., 2012)	Chari–logone Basin	1960–2009	41.35
	20	Our study	Lake Chad Basin	1990–2000	32.41
	21	Our study	Lake Chad Basin	2001–2010	31.71
	22	Our study	Lake Chad Basin	2011–2020	40.94

As a summary of this study, in recent years (far post-drought period), the combined impact of LULC change and climate variability indicated an increase in most of water balance components in LCB and SRB while it shows a decrease in most of water balance components was estimated in NRB. While seperate impact of LULC change indicated an increase in actual ET resulted in the decreases in surface runoff, groundwater recharge, and groundwater return flow in SRB, NRB and LCB. These changes were triggered by the expansion of natural vegetation in the Sahel watersheds and implied a steady reduction in water availability, as well as a limited water recycling in the basin caused by LULC change. The separate impact of climate variability showed that the reduction of precipitation in the NRB augmented the water scarcity, and this could be an alert of desertification in the basin. In the SRB and LCB, the increase in precipitation led to an increase in surface runoff, lateral flow and groundwater return flow. The latter increased potential water recycling and freshwater availability as a consequence of climate variability. This increase in precipitation led to a rise in groundwater recharge as well.

Funding

This work was jointly funded by the project supported by the Key Collaborative Research Program of the Alliance of International Science Organizations (Grant No. ANSO-CR-KP-2022–02), the National Natural Science Foundation of China (NSFC) (Grant No. 42090014, 41661144022), the Chinese Academy of Sciences President's International Fellowship Initiative (Grant No. 2020VTA0001), the MOST High-Level Foreign Expert Program (Grant No. GL20200161002), and the CAS-TWAS President's Fellowship Programme.

CRediT authorship contribution statement

Ali Bennour, Massimo Menenti, Li Jia: Conceptualization, Methodology, Investigation. **Ali Bennour**: Software, Validation, Formal analysis, Writing – original draft preparation. **Li Jia, Massimo Menenti**: Resources. **Ali Bennour, Li Jia, Chaolei Zheng, Min Jiang**: Data curation. **Ali Bennour, Massimo Menenti, Li Jia, Chaolei Zheng, Yelong Zeng, Beatrice Asenso Barnieh, Min Jiang**: Writing – review & editing. **Ali Bennour, Li Jia**: Visualization. **Massimo Menenti, Li Jia**: Supervision. **Li Jia**: Project administration, Funding acquisition. All authors have read and agreed to the published version of the manuscript.

Declaration of Competing Interest

The authors declare that they have no known competing financial interests or personal relationships that could have appeared to influence the work reported in this paper.

Data availability

The data that has been used is available upon requrest.

Appendix

See Figs. A.1-A.4 and Tables A.1-A.5.

Appendix B. Supporting information

Supplementary data associated with this article can be found in the online version at doi:10.1016/j.ejrh.2023.101370.

References

Abbaspour, K.C., 2015, SWAT-CUP SWAT Calibration and Uncertainty Programs - A User Manual, eawag: Swiss Federal Institute of Aquatic Science and Technology.

Aich, V., Liersch, S., Vetter, T., Andersson, J.C.M., Müller, E.N., Hattermann, F.F., 2015. Climate or Land Use?—Attribution of Changes in River Flooding in the Sahel Zone. Water 2796–2820. https://doi.org/10.3390/w7062796.

Albergel, J., 1987, Sécheresse, dbsertification et ressources en eau de surface - Application aux petits bassins du Burkina Faso, The Influence of Climate Change and Climatic Variability on the Hydrologic Regime and Water Resources (Proceedings of the Vancouver Symposium, August 1987). IAHS Publ. no. 168, 1987.

Ali, A., Lebel, T., 2009. The Sahelian standardized rainfall index revisited. Int. J. Climatol. 29 (12), 1705–1714. https://doi.org/10.1002/joc.1832.

Amogu, O., et al., 2015. Evolution de l'écoulement d'un petit bassin-versant sahélien en lien avec les changements d'usage des sols. Hydrol. Sci. J. 60, 78–95. https://doi.org/10.1080/02626667.2014.885654.

Andersen, I., Dione, O., Jaroswich-Holder, M., Olivry, J.C., 2012. The Niger River Basin: AVision for Sustainable Management. Sustain. Healthc. 72–91. https://doi.org/10.1596/978-0-8213-6203-7.

Anyamba, A., Tucker, C.J., 2005. Analysis of Sahelian vegetation dynamics using NOAA-AVHRR NDVI data from 1981–2003. J. Arid Environ. 63 (3), 596–614. https://doi.org/10.1016/j.jaridenv.2005.03.007.

Arnold, J.G., Srinivasan, R., Muttiah, R.S., Williams, J.R., 1998. Large area hydrologic modeling and assessment part I: Model development. J. Am. Water Resour. Assoc. 34, 73–89. https://doi.org/10.1111/j.1752-1688.1998.tb05961.x.

Barnieh, B.A., Jia, L., Menenti, M., Zhou, J., Zeng, Y., 2020. Mapping Land Use Land Cover Transitions at Different Spatiotemporal Scales in West Africa. Sustainability 12 (20), 8565. https://doi.org/10.3390/su12208565.

Barnieh, B.A., Jia, L., Menenti, M., Jiang, M., Zhou, J., Lv, Y., Zeng, Y., Bennour, A., 2022. Quantifying spatial reallocation of land use/land cover categories in West Africa. Ecol. Indic. 135, 108556 https://doi.org/10.1016/j.ecolind.2022.108556.

Bennour, A., Jia, L., Menenti, M., Zheng, C., Zeng, Y., Barnieh, B.A., Jiang, M., 2022. Calibration and validation of SWAT model by using hydrological remote sensing observables in the Lake Chad Basin. Remote Sens. 14, 1511. https://doi.org/10.3390/rs14061511.

Bodian, A., Diop, L., Panthou, G., Dacosta, H., Deme, A., Dezetter, A., Ndiaye, P.M., Diouf, I., Visch, T., 2020. Recent trend in hydroclimatic conditions in the Senegal River basin. Water 12, 1–12. https://doi.org/10.3390/w12020436.

Boulain, N., Cappelaere, B., Séguis, L., Favreau, G., Gignoux, J., 2009. Water balance and vegetation change in the Sahel: A case study at the watershed scale with an eco-hydrological model. J. Arid Environ. 73, 1125–1135. https://doi.org/10.1016/j.jaridenv.2009.05.008.

Brandt, M., Tappan, G., Diouf, A.A., Beye, G., Mbow, C., Fensholt, R., 2017. Woody vegetation die off and regeneration in response to rainfall variability in the west african sahel. Remote Sens. 9, 39. https://doi.org/10.3390/rs9010039.

Casenave, A., Valentin, C., 1992. A runoff capability classification system based on surface features criteria in semi-arid areas of West Africa. J. Hydrol. 130, 231–249. https://doi.org/10.1016/0022-1694(92)90112-9.

Chen, C., Park, T., Wang, X., Piao, S., Xu, B., Chaturvedi, R.K., Fuchs, R., Brovkin, V., Ciais, P., Fensholt, R., Tømmervik, H., Bala, G., Zhu, Z., Nemani, R.R., Myneni, R. B., 2019. China and India lead in greening of the world through land-use management. Nat. Sustain. 2, 122–129. https://doi.org/10.1038/s41893-019-0220-7.

Chen, Y.-R., Yu, B., 2013. Impacts of climate and land-use changes on floods in an urban catchment in southeast Queensland, Australia. IAHS-AISH Proceedings and Reports, 359, pp. 425–429.

Chu, H.-j, Lin, Y.-p, Huang, C.-w, Hsu, C.-y, Chen, H.-y, 2010. Modelling the hydrologic effects of dynamic land-use change using a distributed hydrologic model and a spatial land-use allocation model, 2554, 2538–2554. https://doi.org/10.1002/hyp.7667.

Daramola, J., Adepehin, E.J., Ekhwan, T.M., Choy, L.K., Mokhtar, J., Tabiti, T.S., 2022. Impacts of land-use change, associated land-use area and runoff on watershed sediment yield: implications from the Kaduna Watershed. Water 14 (3), 325. https://doi.org/10.3390/w14030325.

Dardel, C., Kergoat, L., Hiernaux, P., Grippa, M., Mougin, E., Ciais, P., Nguyen, C.C., 2014. Rain-Use-Efficiency: What it Tells us about the Conflicting Sahel Greening and Sahelian Paradox. Remote Sens. 6 (4), 3446–3474. https://doi.org/10.3390/rs6043446.

Delclaux, F., Le Coz, M., Coe, M., G., F., Ngounou N.B., 2008, Confronting Models with Observations for evaluating Hydrological Change in the Lake Chad Basin, Africa, Confronting Models with Observations for evaluating Hydrological Change in the Lake Chad Basin, Africa, Montpellier, France.

Descroix, L., Genthon, P., Amogu, O., Rajot, J.L., Sighomnou, D., Vauclin, M., 2012. Change in Sahelian Rivers hydrograph: The case of recent red floods of the Niger River in the Niamey region. Glob. Planet. Change 98–99, 18–30. https://doi.org/10.1016/j.gloplacha.2012.07.009.

Descroix, L., , et al.Diongue Niang, A., Panthou, G., Bodian, A., Sane, Y., Dacosta, H., Malam Abdou, M., Vandervaere, J.P., Quantin, G., 2015. Recent trend on rainfall in West Africa through two regions: Senegambia and the Middle Niger River Basin. Climatologie 12, 25–43. https://doi.org/10.4267/climatologie.1105.

Descroix, L., Mahé, G., Lebel, T., Favreau, G., Galle, S., Gautier, E., Olivry, J.C., Albergel, J., Amogu, O., Cappelaere, B., Dessouassi, R., Diedhiou, A., Le Breton, E., Mamadou, I., Sighomnou, D., 2009. Spatio-temporal variability of hydrological regimes around the boundaries between Sahelian and Sudanian areas of West Africa: A synthesis. J. Hydrol. 375, 90–102. https://doi.org/10.1016/j.jhydrol.2008.12.012.

Descroix, L., Guichard, F., Grippa, M., Lambert, L.A., Panthou, G., Mahé, G., Gal, L., Dardel, C., Quantin, G., Kergoat, L., Bouaïta, Y., Hiernaux, P., Vischel, T., Pellarin, T., Faty, B., Wilcox, C., Abdou, M.M., Mamadou, I., Vandervaere, J.P., Diongue-Niang, A., Ndiaye, O., Sané, Y., Dacosta, H., Gosset, M., Cassé, C., Sultan, B., Barry, A., Amogu, O., Nnomo, B.N., Barry, A., Paturel, J.E., 2018. Evolution of surface hydrology in the Sahelo-Sudanian Strip: An updated review. Water 10. https://doi.org/10.3390/w10060748.

Diop, L., Yaseen, Z.M., Bodian, A., Djaman, K., Brown, L., 2017. Trend analysis of streamflow with different time scales: a case study of the upper Senegal River. ISH J. Hydraul. Eng. 24 (1), 105–114. https://doi.org/10.1080/09715010.2017.1333045.

Draper, C.S., Walker, J.P., Steinle, P.J., de Jeu, R.A.M., Holmes, T.R.H., 2009. An evaluation of AMSR-E derived soil moisture over Australia. Remote Sens. Environ. 113, 703–710. https://doi.org/10.1016/j.rse.2008.11.011.

Ewen, J., Parkin, G., 1995. Validation of catchment models for predicting land-use and climate change impacts. 3. Blind validation for internal and outlet responses. J. Hydrol. 287, 74–94. https://doi.org/10.1016/j.jhydrol.2003.09.021.

Faty, A., Kouame, F., Niang Fall, A., Kane, A., 2019. Land use dynamics in the context of variations in hydrological regimes in the upper Senegal River basin. Int. J. Hydrol. 3, 185–192. https://doi.org/10.15406/ijh.2019.03.00179.

Favreau, G., Cappelaere, B., Massuel, S., Leblanc, M., Boucher, M., Boulain, N., Leduc, C., 2009. Land clearing, climate variability, and water resources increase in semiarid southwest Niger: A review. Water Resour. Res. 45 (7) https://doi.org/10.1029/2007wr006785.

Faye, B., Du, G., 2021. Agricultural Land Transition in the "Groundnut Basin" of Senegal: 2009 to 2018. Land 10 (10), 996. https://doi.org/10.3390/land10100996.

Feng, D., Yu, L., Zhao, Y., Cheng, Y., Xu, Y., Li, C., Gong, P., 2018. A multiple dataset approach for 30-m resolution land cover mapping: a case study of continental Africa. Int. J. Remote Sens. 39 (12), 3926–3938. https://doi.org/10.1080/01431161.2018.1452073.

Fensholt, R., Rasmussen, K., 2011. Analysis of trends in the Sahelian 'rain-use efficiency' using GIMMS NDVI, RFE and GPCP rainfall data. Remote Sens. Environ. 115 (2), 438–451. https://doi.org/10.1016/j.rse.2010.09.014.

Feyen, J., Vázquez, R., 2011. Modeling hydrological consequences of climate and land use change - Progress and Challenges. Maskana 2, 83–100. https://doi.org/10.18537/mskn.02.02.07.

Giertz, S., Junge, B., Diekkrüger, B., 2005. Assessing the effects of land use change on soil physical properties and hydrological processes in the sub-humid tropical environment of West Africa. Phys. Chem. Earth, Parts A/B/C. 30 (8–10), 485–496. https://doi.org/10.1016/j.pce.2005.07.003.

Guzha, A.C., Rufino, M.C., Okoth, S., Jacobs, S., Nóbrega, R.L.B., 2018. Impacts of land use and land cover change on surface runoff, discharge and low flows: Evidence from East Africa. J. Hydrol.: Reg. Stud. 49–67. https://doi.org/10.1016/j.ejrh.2017.11.005.

Hersbach, H., Bell, B., Berrisford, P., Hirahara, S., Horányi, A., Muñoz-Sabater, J., Nicolas, J., Peubey, C., Radu, R., Schepers, D., Simmons, A., Soci, C., Abdalla, S., Abellan, X., Balsamo, G., Bechtold, P., Biavati, G., Bidlot, J., Bonavita, M., De Chiara, G., Dahlgren, P., Dee, D., Diamantakis, M., Dragani, R., Flemming, J., Forbes, R., Fuentes, M., Geer, A., Haimberger, L., Healy, S., Hogan, R.J., Hólm, E., Janisková, M., Keeley, S., Laloyaux, P., Lopez, P., Lupu, C., Radnoti, G., de Rosnay, P., Rozum, I., Vamborg, F., Villaume, S., Thépaut, J.N., 2020. The ERA5 global reanalysis. Q. J. R. Meteorol. Soc. 146, 1999–2049. https://doi.org/10.1002/qj.3803.

Hollis, G.E., 1990, Senegal River Basin Monitoring Activity: Hydrological Issues: Part II, Institute for Development Anthropology, Binghamton, NY, USA.

Hu, G., Jia, L., 2015. Monitoring of evapotranspiration in a semi-arid inland river basin by combining microwave and optical remote sensing observations. Remote Sens. 7, 3056–3087. https://doi.org/10.3390/rs70303056.

Hulme, M., 2001. Climatic perspectives on Sahelian desiccation: 1973–1998. Global Environmental Change 11, 19–29. https://doi.org/10.1016/S0959-3780(00)00042-X.

Jia, L., Zheng, C., Hu, G.C., Menenti, M., 2018. Evapotranspiration, in Comprehensive Remote Sensing. In: Liang, S. (Ed.). Elsevier, Oxford, pp. 25–50. https://doi.org/10.1016/B978-0-12-409548-9.10353-7.

Jiang, M., Jia, L., Menenti, M., Zeng, Y., 2022. Understanding spatial patterns in the drivers of greenness trends in the Sahel-Sudano-Guinean region. Big Earth Data. https://doi.org/10.1080/20964471.2022.2146632.

Karambiri, H., García Galiano, S.G., Giraldo, J.D., Yacouba, H., Ibrahim, B., Barbier, B., Polcher, J., 2011. Assessing the impact of climate variability and climate change on runoff in West Africa: The case of Senegal and Nakambe River basins. Atmos. Sci. Lett. 12, 109–115. https://doi.org/10.1002/asl.317.

Kouchi, D.H., Esmaili, K., Faridhosseini, A., Sanaeinejad, S.H., Khalili, D., Abbaspour, K.C., 2017. Sensitivity of calibrated parameters and water resource estimates on different objective functions and optimization algorithms. Wate 9, 1–16. https://doi.org/10.3390/w9060384.

L. Descroix I. Bouzou Moussa P. Genthon D. Sighomnou G. Mahé I. Mamadou J.P. Vandervaere E. Gautier O. Faran Maiga J.-L. Rajot M. Malam Abdou N. Dessay A. Ingatan I. Noma K. Souley Yéro H. Karambiri R. Fensholt J. Albergel J. Olivry Impact of Drought and Land – Use Changes on Surface – Water Quality and Quantity: The Sahelian Paradox InTech, Zagreb 2013 Croatie 243 271 doi: 10.5772/54536.Chapter10.

Leblanc, M.J., Favreau, G., Massuel, S., Tweed, S.O., Loireau, M., Cappelaere, B., 2008. Land clearance and hydrological change in the Sahel. SW Niger. Global and Planetary Change 61, 135–150. https://doi.org/10.1016/j.gloplacha.2007.08.011.

Leduc, C., Favreau, G., Schroeter, P., 2001. Long-term rise in a Sahelian water-table: the Continental Terminal in South-West Niger. Journal of Hydrology, 243: 43–54. DOI:10.1016/S0022-1694(00)00403-0.

Lemoalle, J., Bader, J.C., Leblanc, M., Sedick, A., 2012. Recent changes in Lake Chad: Observations, simulations and management options (1973-2011). Glob. Planet. Change 80–81, 247–254. https://doi.org/10.1016/j.gloplacha.2011.07.004.

Lopez, L.P., Sutanudjaja, E., Schellekens, J., Sterk, G., Bierkens, M., 2017. Calibration of a large-scale hydrological model using satellite-based soil moisture and evapotranspiration products. Hydrol. Earth Syst. Sci. 1–39. https://doi.org/10.5194/hess-2017-16.

Lørup, J.K., Refsgaard, J.C., Mazvimavi, D., 1998. Assessing the effect of land use change on catchment runoff by combined use of statistical tests and hydrological modelling: Case studies from Zimbabwe. J. Hydrol. 54, 147–163. https://doi.org/10.1007/s11434-008-0538-4.

Mahamat Nour, A., Vallet-Coulomb, C., Gonçalves, J., Sylvestre, F., Deschamps, P., 2021. Rainfall-discharge relationship and water balance over the past 60 years within the Chari-Logone sub-basins, Lake Chad basin. J. Hydrol.: Reg. Stud. 35, 100824 https://doi.org/10.1016/j.ejrh.2021.100824.

Mahe, G., 2006, The impacts of land-use/land-cover change and climate variability on the hydrology of the Sahel. IAHS-AISH Publication: 679–684.

Mahe, G., Olivry, J.-C., 1999. Assessment of freshwater yields to the ocean along the inter- tropical Atlantic coast of Africa. Earth and Planetary Sciences 328, 621–626. https://doi.org/10.1016/S1251-8050(99)80159-1.

Mahé, G., Paturel, J.E., 2009. 1896-2006 Sahelian annual rainfall variability and runoff increase of Sahelian Rivers. Comptes Rendus - Geosci. 341, 538–546. https://doi.org/10.1016/j.crte.2009.05.002.

Mahe, G., Leduc, C., Amani, A., Paturel, J.-E., Girard, S., Seryat, E., Dezetter, A., 2003, Augmentation récente du ruissellement de surface en région soudano-sahélienne et impact sur les ressources en eau, Hydrology of the Mediterranean and Semi-Arid Regions, proceedings of an international symposium. Wallingford, UK, IAHS, Montpellier (France), pp. 215–222.

Mahe, G., Lienou, G., Bamba, F., Paturel, J.E., Adeaga, O., Descroix, L., Mariko, A., Olivry, J.C., Sangare, S., Ogilivie, A., Clanet, J.C., 2011, Le fleuve Niger et le changement climatique au cours des 100 dernières années, Hydro-climatology: Variability and Change (Proceedings of symposium J-H02 held during IUGG2011 in Melbourne, Australia, July 2011) (IAHS Publ. 344, 2011).

Mahmood, R., Jia, S., 2019. Assessment of hydro-climatic trends and causes of dramatically declining stream flow to Lake Chad, Africa, using a hydrological approach. Sci. Total Environ. 675, 122–140. https://doi.org/10.1016/j.scitotenv.2019.04.219.

Mamadou, I., Gautier, E., Descroix, L., Noma,, I., Bouzou Moussa, I., Faran Maiga, O., Genthon, P., Amogu, O., Malam Abdou, M., Vandervaere, J.P., 2015. Exorheism growth as an explanation of increasing flooding in the Sahel. Catena 131, 130–139. https://doi.org/10.1016/j.catena.2015.03.017.
Mao, D., Cherkauer, K.A., 2009. Impacts of land-use change on hydrologic responses in the Great Lakes region. J. Hydrol. 374, 71–82. https://doi.org/10.1016/j.jhydrol.2009.06.016.
Marshall, M., Funk, C., Michaelsen, J., 2012. Examining evapotranspiration trends in Africa. Clim. Dyn. 38, 1849–1865. https://doi.org/10.1007/s00382-012-1299-y.
Moriasi, D.N., Gitau, M.W., Pai, N., Daggupati, P., 2015. Hydrologic and water quality models: Performance measures and evaluation criteria. Am. Soc. Agric. Biol. Eng. 58, 1763–1785. https://doi.org/10.13031/trans.58.10715.
Moriasi, D.N., Arnold, J.G., Van Liew, M.W., Bingner, R.L., Harmel, R.D., Veith, T.L., 2007. Model evaluation guidelines for systematic quantification of accuracy in watershed simulations. Am. Soc. Agric. Biol. Eng. 50, 885–900. https://doi.org/10.13031/2013.23153.
Mounirou, L.A., Zouré, C.O., Yonaba, R., Paturel, J.-E., Mahé, G., 2020. Multi-scale analysis of runoff from a statistical perspective in a small Sahelian catchment under semi-arid climate. Arabian Journal of Geosciences 13. https://doi.org/10.1007/s12517-020-5141-2.
Neitsch, S.L., Arnold, J.G., Kiniry, J.R., Williams, J.R., 2011, Soil & Water Assessment Tool Theoretical Documentation Version 2009; Texas Water Resources Institute, Texas, USA.
Nka, B.N., Oudin, L., Karambiri, H., Paturel, J.E., Ribstein, P., 2015. Trends in floods in West Africa: analysis based on 11 catchments in the region. Hydrol. Earth Syst. Sci. 19 (11), 4707–4719. https://doi.org/10.5194/hess-19-4707-2015.
Nkiaka, E., Nawaz, N.R., Lovett, J.C., 2017. Analysis of rainfall variability in the Logone catchment, Lake Chad basin. Int. J. Climatol. 37 (9), 3553–3564. https://doi.org/10.1002/joc.4936.
Nwilo, P.C., Olayinka, D.N., Okolie, C.I., Emmanuel, E.I., Orji, M.I., Daramola, O.E., 2020. Impacts of land cover changes on desertification in northern Nigeria and implications on the Lake Chad Basin. J. Arid Environ. 181, 104190 https://doi.org/10.1016/j.jaridenv.2020.104190.
Obahoundje, S., Diedhiou, A., 2022. Potential impacts of climate, land use and land cover changes on hydropower generation in West Africa: a review. Environ. Res. Lett. 17 (4), 043005 https://doi.org/10.1088/1748-9326/ac5b3b.
Odusanya, A.E., Mehdi, B., Schürz, C., Oke, A.O., Awokola, O.S., Awomeso, J.A., Adejuwon, J.O., Schulz, K., 2019. Multi-site calibration and validation of SWAT with satellite-based evapotranspiration in a data-sparse catchment in southwestern Nigeria. Hydrol. Earth Syst. Sci. 23 (2), 1113–1144. https://doi.org/10.5194/hess-23-1113-2019.
Ogutu, B.O., D'Adamo, F., Dash, J., 2021. Impact of vegetation greening on carbon and water cycle in the African Sahel-Sudano-Guinean region. Glob. Planet. Change 202, 103524. https://doi.org/10.1016/j.gloplacha.2021.103524.
Okonkwo, C., Demoz, B., Gebremariam, S., 2014. Characteristics of Lake Chad level variability and links to ENSO, precipitation, and river discharge. ScientificWorldJournal 2014, 145893. https://doi.org/10.1155/2014/145893.
Okpara, J.N., Tarhule, A.A., Perumal, M., 2013. Study of Climate Change in Niger River Basin, West Africa: Reality Not a Myth. In: Singh, B.R. (Ed.), Climate Change – Realities, Impacts Over Ice Cap, Sea Level and Risks. https://doi.org/10.5772/55186.
Olsson, L., Eklundh, L., Ardö, J., 2005. A recent greening of the Sahel—trends, patterns and potential causes. J. Arid Environ. 63 (3), 556–566. https://doi.org/10.1016/j.jaridenv.2005.03.008.
Op de Hipt, F., Diekkruger, B., Steup, G., Yira, Y., Hoffmann, T., Rode, M., Naschen, K., 2019. Modeling the effect of land use and climate change on water resources and soil erosion in a tropical West African catch-ment (Dano, Burkina Faso) using SHETRAN. Sci. Total Environ. 653, 431–445. https://doi.org/10.1016/j.scitotenv.2018.10.351.
Oyebande, L., Odunuga, S., 2010. Climate Change Impact on Water Resources at the Transboundary Level in West Africa: The Cases of the Senegal, Niger and Volta Basins. The Open Hydrology Journal 4, 163–172. https://doi.org/10.2174/1874378101004010163.
P. Yao S. Jiancheng Z. Tianjie K. Yang M.H. Cosh D.J.S. Gianotti D. Entek A long term global daily soil moisture dataset derived from AMSR-E and AMSR2 (2002 – 2019) 2021 1 16 doi: 10.1038/s41597–021-00925–8.
Pham-Duc, B., Sylvestre, F., Papa, F., Frappart, F., Bouchez, C., Crétaux, J.F., 2020. The Lake Chad hydrology under current climate change. Scientific Reports. 10, 1–10. https://doi.org/10.1038/s41598-020-62417-w.
Poméon, T., Diekkrüger, B., Springer, A., Kusche, J., Eicker, A., 2018. Multi-objective validation of SWAT for sparsely-gaugedWest African river basins - A remote sensing approach. Water (Switz.) 10. https://doi.org/10.3390/w10040451.
Rajib, M.A., Merwade, V., Yu, Z., 2016. Multi-objective calibration of a hydrologic model using spatially distributed remotely sensed/in-situ soil moisture. J. Hydrol. 536, 192–207. https://doi.org/10.1016/j.jhydrol.2016.02.037.
Rameshwaran, P., Bell, V.A., Davies, H.N., Kay, A.L., 2021. How might climate change affect river flows across West Africa. Clim. Change 169 (3–4). https://doi.org/10.1007/s10584-021-03256-0.
Sane, M.L., Sambou, S., Leye, I., Ndione, D.M., Diatta, S., Ndiaye, I., Badji, M.L., Kane, S., 2020. Calibration and Validation of the SWAT Model on the Watershed of Bafing River, Main Upstream Tributary of Senegal River: Checking for the Influence of the Period of Study. Open J. Mod. Hydrol. 10, 81–104. https://doi.org/10.4236/ojmh.2020.104006.
Scott, G., Rajabifard, A., 2017. Sustainable development and geospatial information: a strategic framework for integrating a global policy agenda into national geospatial capabilities. Geo-Spat. Inf. Sci. 20 (2), 59–76. https://doi.org/10.1080/10095020.2017.1325594.
Sighomnou, D., Descroix, L., Genthon, P., Mahé, G., Bouzou Moussa, I., Gautier, E., Mamadou, I., Vandervaere, J.-P., Bachir, T., Coulibaly, B., Rajot, I.-L., Malam Issa, O., Malam Abdou, M., Dessay, N., Delaitre, E., Maiga, O.F., Diedhiou,, A., Panthou, G., Vischel, T., Yacouba, H., Karambiri, H., Paturel, J.-E., Diello, P., Mougin, E., Kergoat, L., Hiernaux, P., 2013. The Niger River Niamey flood of 2012: The paroxysm of the Sahelian paradox. Sécheresse 24 (1), 3–13. https://doi.org/10.1684/sec.2013.0370.
Sun, L., Nistor, I., Seidou, O., Sambou, S., Kebe, C., Tamba, S., 2013, Prediction of daily discharge at Bakel (Senegal) using multiple linear regression, Kalman Filer and Artificial Neural Networks. *CSCE 2013, 3rd Specialty Conference on Disaster Prevention and Mitigation*. Montreal. 2: 1466–1474.
Trémolières, M., 2010, Security and environmental variables: The debate and an analysis of links in the Sahel. Paris: Organisation for Economic Co-operation and Development (OECD).
Trichon, V., Hiernaux, P., Walcker, R., Mougin, E., 2018. The persistent decline of patterned woody vegetation: The tiger bush in the context of the regional Sahel greening trend. Glob. Change Biol. 24, 2633–2648. https://doi.org/10.1111/gcb.14059.
Vinuesa, R., et al., 2020. The role of artificial intelligence in achieving the Sustainable Development Goals. Nat. Commun. 11 (1), 233. https://doi.org/10.1038/s41467-019-14108-y.
Vittek, M., Brink, A., Donnay, F., Simonetti, D., Desclée, B., 2014. Land Cover Change Monitoring Using Landsat MSS/TM Satellite Image Data over West Africa between 1975 and 1990. Remote Sens. 6 (1), 658–676. https://doi.org/10.3390/rs6010658.
Wilcox, C., Vischel, T., Panthou, G., Bodian, A., Blanchet, J., Descroix, L., Quantin, G., Cassé, C., Tanimoun, B., Kone, S., 2018. Trends in hydrological extremes in the Senegal and Niger Rivers. J. Hydrol. 566, 531–545. https://doi.org/10.1016/j.jhydrol.2018.07.063.
Xu, Y., , et al.Yu, L., Zhao, F.R., Cai, X., Zhao, J., Lu, H., Gong, P., 2018. Tracking annual cropland changes from 1984 to 2016 using time-series Landsat images with a change-detection and post-classification approach: Experiments from three sites in Africa. Remote Sens. Environ. 218, 13–31. https://doi.org/10.1016/j.rse.2018.09.008.
Yin, Z., Feng, Q., Yang, L., Wen, X., Si, J., Zou, S., 2017. Long term quantification of climate and land cover change impacts on streamflow in an alpine river catchment, northwestern China. Sustain 9. https://doi.org/10.3390/su9071278.
Yonaba, R., et al., 2021. A dynamic land use/land cover input helps in picturing the Sahelian paradox: Assessing variability and attribution of changes in surface runoff in a Sahelian watershed. Sci. Total Environ. 757, 143792 https://doi.org/10.1016/j.scitotenv.2020.143792.
Yu, L., 2022. 30m land use and cover maps for the Sahel-Sudano-Guinean region of Africa (1990-2020). National Tibetan Plateau/Third Pole Environment Data. Center, National Tibetan Plateau/Third Pole Environment Data Center.
Zhao, J., Yu, L., Liu, H., Huang, H., Wang, I., Gong, P., 2021. Towards an open and synergistic framework for mapping global land cover. PeerJ 9, e11877. https://doi.org/10.7717/peerj.11877.

Zheng, C., Jia, L., 2020. Global canopy rainfall interception loss derived from satellite earth observations. Ecohydrology 13 (2). https://doi.org/10.1002/eco.2186.
Zheng, C., Jia, L., Hu, G., 2022. Global land surface evapotranspiration monitoring by ETMonitor model driven by multi-source satellite earth observations. J. Hydrol. 613, 128444 https://doi.org/10.1016/j.jhydrol.2022.128444.
Zhu, W., Yan, J., Jia, S., 2017. Monitoring recent fluctuations of the southern pool of lake chad using multiple remote sensing data: Implications for water balance analysis. Remote Sens. 9. https://doi.org/10.3390/rs9101032.
Zhu, W., Jia, S., Lall, U., Cao, Q., Mahmood, R., 2019. Relative contribution of climate variability and human activities on the water loss of the Chari/Logone River discharge into Lake Chad: A conceptual and statistical approach. J. Hydrol. 569, 519–531. https://doi.org/10.1016/j.jhydrol.2018.12.015.